

AE-511

UDC 533.6.011:
661.91
532.51

AE-511

Methods for Sampling and Measurement of Compressed Air Contaminants

L. Ström



AKTIEBOLAGET ATOMENERGI

STUDSVIK, NYKÖPING, SWEDEN 1976

METHODS FOR SAMPLING AND MEASUREMENT
OF COMPRESSED AIR CONTAMINANTS

Lars Ström

SYNOPSIS

In order to improve the technique for measuring oil and water entrained in a compressed air stream, a laboratory study has been made of some methods for sampling and measurement. For this purpose water or oil as artificial contaminants were injected in thin streams into a test loop, carrying dry compressed air. Sampling was performed in a vertical run, down-stream of the injection point. Wall-attached liquid, coarse droplet flow, and fine droplet flow were sampled separately. The results were compared with two-phase flow theory and direct observation of liquid behaviour.

In a study of sample transport through narrow tubes, it was observed that, below a certain liquid loading, the sample did not move, the liquid remaining stationary on the tubing wall.

The basic analysis of the collected samples was made by gravimetric methods. Adsorption tubes were used with success to measure water vapour. A humidity meter with a sensor of the aluminium oxide type was found to be unreliable. Oil could be measured selectively by a flame ionization detector, the sample being pretreated in an evaporation-condensation unit.

Printed and distributed in October 1976

ISBN-91-7010-007-1

CONTENTS

	page
PREFACE	2
1. INTRODUCTION	3
2. SAMPLING	7
2.1 Principles	7
2.2 Character of flow	7
2.3 Wall flow sampler	11
2.4 Coarse air-borne liquid sampler	16
2.5 Gas and fine air-borne liquid sampler	21
2.6 Conclusions concerning samplers	23
2.7 Calculation of vapour and liquid flows from sample flows	24
3. SAMPLE TRANSPORT	24
3.1 Estimation of transport velocity	26
3.2 Experiments on transport velocity	27
4. SAMPLE PREPARATION	28
4.1 Requirements regarding sample flow to instruments	28
4.2 Mechanical homogenization of sample flow	30
4.3 Sample vaporization	31
4.4 Evaporator	34
4.5 Condensation unit	35
5. INSTRUMENTS	37
5.1 Investigated methods	37
5.2 Humidity measurement	37
5.3 Hydrocarbon measurement	39
6. NOTES ON CONTINUED INVESTIGATIONS	43
7. REFERENCES	45

PREFACE

The investigation reported here was initiated by the Swedish Association of Metal Working Industries, Working Group for Fluid Systems Technology.

The project has been directed by a committee with the following members:

I Ahlberg	AB Westin & Backlund
K C Blomqvist	AB Mecman (part-time)
B Granström	Atlas Copco AB
L Innings	AB Mecman (part-time)
O Möre	L M Ericsson AB (part-time)
L Ström	AB Atomenergi (project leader)

Laboratory work has been performed by G Gebert and A Dahlgren of AB Atomenergi.

The project has received financial support from the Swedish Board for Technical Development.

This report is also published in the publication series of the Swedish Association of Metal Working Industries.

1. INTRODUCTION

Most compressed air applications require a limit to be set on the amount of contaminants in the air stream. Also the air may carry a lubricant, which is necessary for the operation of an air-driven tool. In such a case the application also demands that a lower limit is set on the amount of oil. But too much oil may lead to contamination of the air at the workplace. It accordingly becomes evident that technical, economical and occupational health aspects combine to require well-defined contamination* levels in different applications. This situation has been recognized by the International Organization for Standardization (ISO) which has formed a committee for the standardization of compressed air quality (Technical Committee 118, Working Group 2: Quality of compressed air and influence on environment from the use of pneumatic equipment).

Some standardization of compressed air has already been carried out (ref 22, 24, 25), but it is relevant only to cylinder air.

The necessary measurement technique has received little attention. Only a few relevant publications have been found (ref 14, 20, 21, 22, 26). Of these, the dissertations of Sittel and Munro are the most important. They have both studied oil mist lubrication. The difficulties of sampling were avoided by measuring droplets optically in the pressurized conduit. A large body of data on oil droplet generation and transmission is reported.

The publications by Evans and from CGA are concerned with cylinder air, and the observations of these papers are not of immediate interest in this context.

The project reported here was undertaken with the main objective to improve the measurement technique. It is desirable to develop methods which can be applied in the field without recourse to skilled personnel and laboratory facilities. Measurements should preferably be presented as continuous recordings.

* For the sake of simplicity the term "contamination" is used here for any liquid or vapour in the air stream, whether its presence is intentional or not.

Measurement range

Compressed air is used for many purposes, with widely different tolerance to contamination. To limit the scope of this investigation, medical and food processing applications were excluded, and also breathing air. Particles were not regarded as important. Still, the range of the parameters to be covered is considerable. The following contaminant limits were set, to comprise most industrial applications:

TABLE 1:1

Contaminant limits		
Water as liquid	300 - 1,000 mg/m ³ (Norm)*	
Water as vapour	10 - 3,000 "	"
Oil as liquid	10 - 1,000 "	"

The maximum liquid water concentration corresponds to a compressor with an aftercooler and a cyclone water separator. The minimum water vapour concentration corresponds to a dew point at atmospheric pressure of about -55°C.

The upper limit of the oil range can occur at oil mist lubrication, while the lower concentration can describe "oil-free air" in many applications.

The vapour concentration of oil is not specified. Lubricating oil has a very low vapour pressure at room temperature, see Figure 4.2. Some information on oil concentration can be found in ref 19.

The air flow varies considerably from small air tools to large compressors. The flow of contaminant varies under these conditions over more than four decades, Figure 1.1. It has not been possible to cover this large dynamic range in one set of equipment.

Nature of contaminants

Particles of sand, rust, scale, etc may be destructive to pneumatic equipment. But as already mentioned; they are left out of consider-

* "Norm" implies that the volume is referred to the standard conditions of 101325 Pa (760 mm Hg) and 20°C.

ration in this investigation, mainly because the measurement technique is very different from the technique for liquids and vapours.

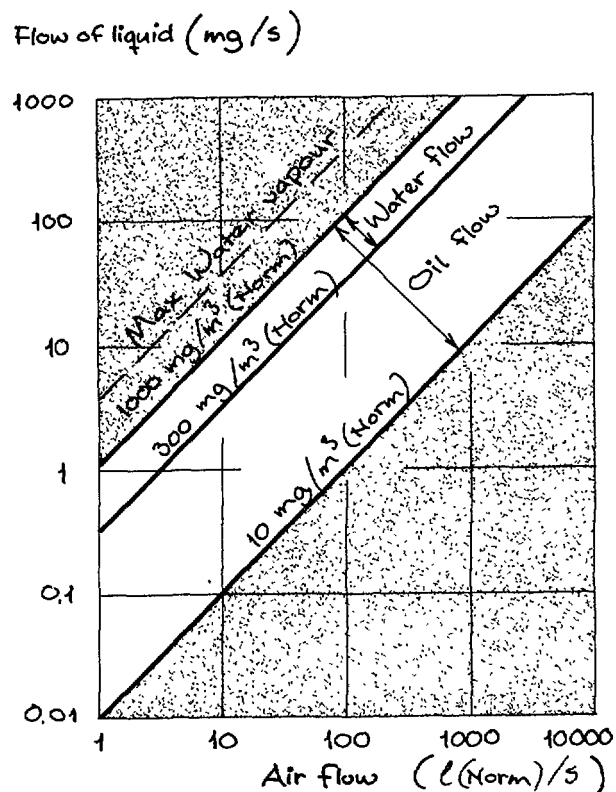


Fig 1.1 Assumed contamination concentration and flow for liquid water and oil.

The oil in compressed air is mainly of two kinds: compressor oil and air tool oil. In our experiments we have used both, Table 1:2.

TABLE 1:2 SPECIFICATIONS OF OILS EMPLOYED

Designation in this report	O	N
Manufacturer	Oljekonsumenterna	Nynäs-Petroleum
Manufacturer's designation	K-14	Compressor oil 35
Density, kg/m ³	870 (20°C)	875 (15°C)
	{ 35 (20°C)	58 (38°C)
Viscosity, c St	{ 11.2 (50°C)	
	{ 3.6 (99°C)	7.6 (99°C)

Test loop

To facilitate experiments on sampling technique, a test loop was set up in the laboratory as shown in Figure 1.2. The loop consists of one vertical and two horizontal sections of stainless steel tubing, internal diameter 16 mm. In the first horizontal section, oil and water can be injected into the dried, filtered, and pressure-regulated air stream. Filter penetration is stated by the manufacturer to be less than 10^{-5} for submicron particles.

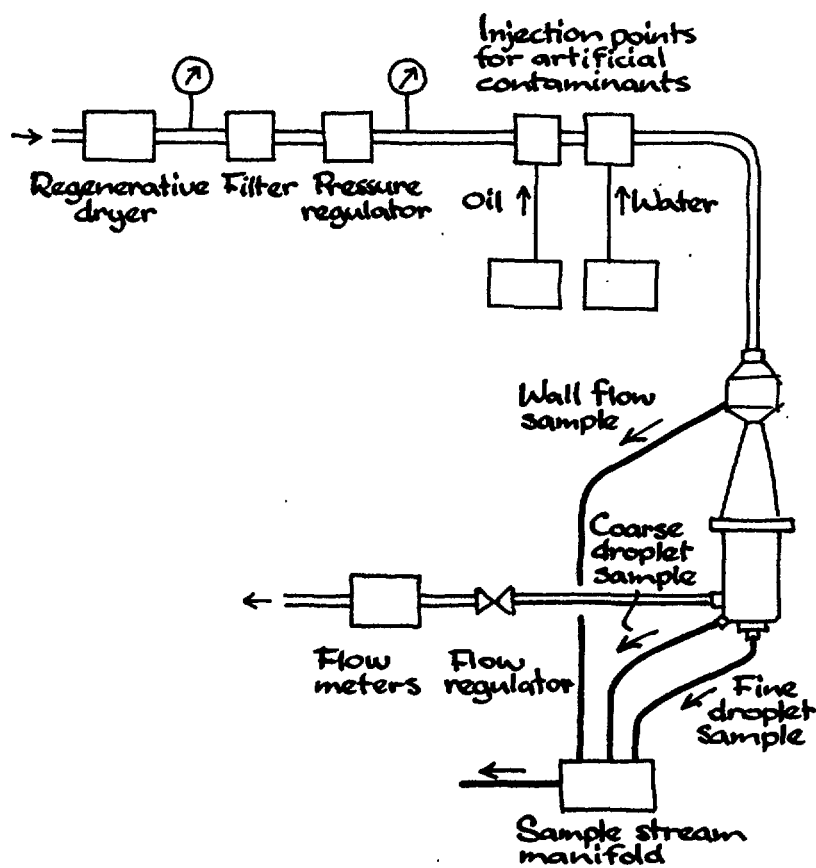


Fig 1.2 Compressed air loop for investigation of sampling and sample transport.

Different sampling devices are being tested in the vertical section. The vertical part before the samplers is c 400 mm long.

The air flow is measured and regulated in the second horizontal section. The pressure is usually kept constant at 600 kPa above atmospheric pressure.

2. SAMPLING

2.1 Principles

The flow of contaminants may appear as liquid flowing on the conduit walls, as free droplets in the air stream, or as vapour. Sampling of wall-attached liquid and of coarse droplets must be done by complete extraction, because it is impossible to make sure that any partial flow is representative. On the other hand, vapour and fine particles cannot be extracted completely and made available at a measuring instrument. But for these fractions a representative partial flow can be withdrawn, under suitable precautions. Thus in order to measure the contaminant flow in all of its phases, the two categories wall-attached flow and coarse air borne droplets, and fine air-borne droplets and vapour, must be separately sampled.

2.2 Character of flow

To gain a better foundation for the design of samplers, a study has been made of liquid-in-air flow.

A mixed stream of gas and liquid is a case of two-phase flow. Because of its importance in some engineering applications (heat transfer, gas-liquid reactions) it has received considerable attention, from a practical as well as from a theoretical point of view (refs 3, 6, 8, 9).

The mode of flow is influenced by the properties of the liquid, the gas, and the conduit. This is illustrated by the well-known Baker diagram (ref 2, ref 3 p 727), showing observed flow patterns in a horizontal circular tube. To incorporate the very low liquid flows of interest here, the diagram has been extended to low flows, Figure 2.1. The contaminant flow limits expressed by Table 1:1, and common air flows per unit area in compressed air conduits form the boundaries of the region of interest. The region is drawn as a rectangle in Figure 2.1 (marked - · - · -).

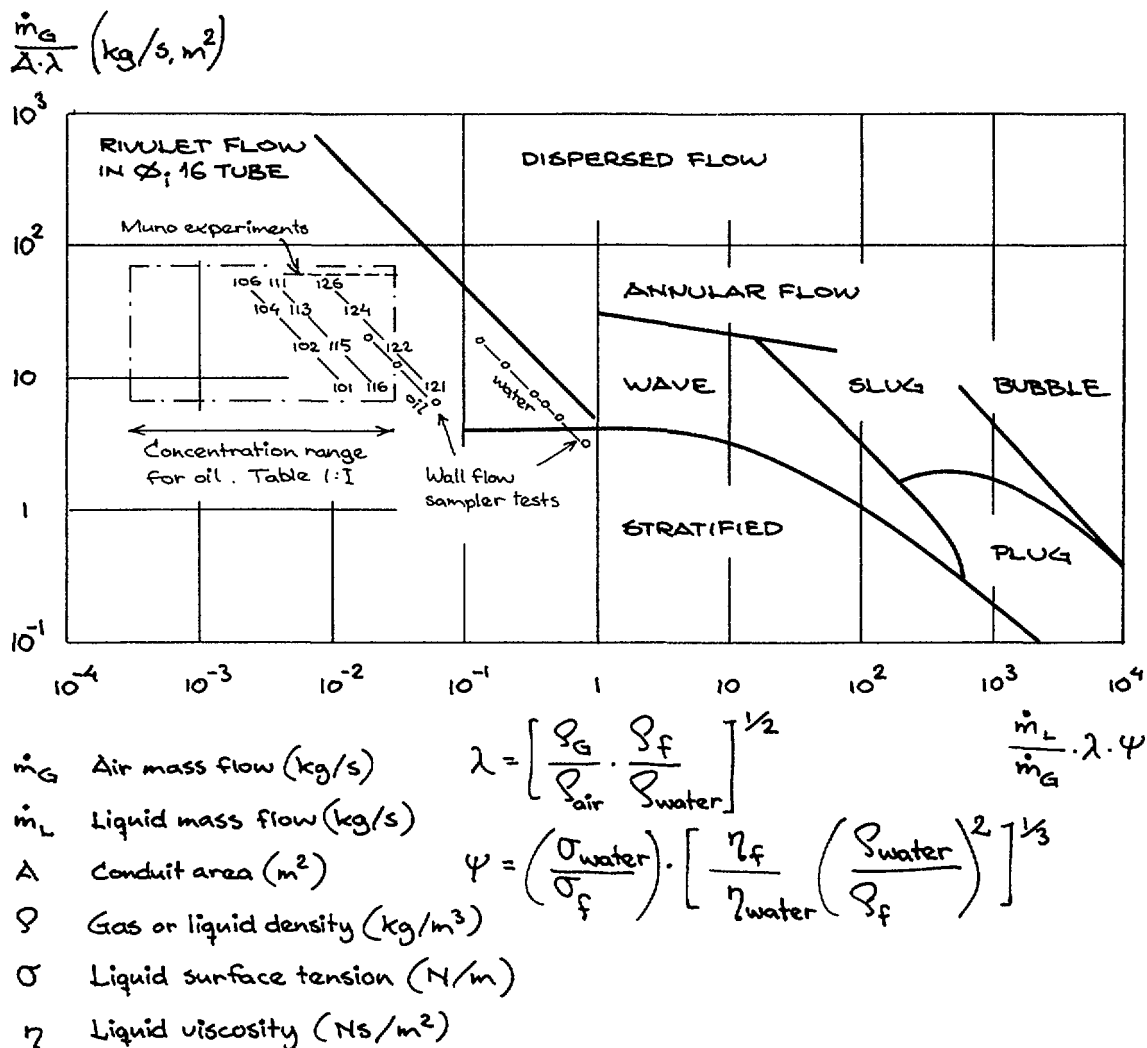


Fig 2.1 Baker diagram showing flow modes in a horizontal tube.

By means of the Baker diagram it is possible to compare results from experiments made under different conditions of liquid surface tension, viscosity and density, and gas density. Other similar correlations are discussed in ref 6.

Results applying to low liquid flows are very sparse. Levy (ref 12) has derived expressions for film thickness and liquid entrainment into the core. These data extend to rather thin films, less than 1 % of pipe radius. At a low liquid flow the film breaks up into thin streams, termed rivulets. According to Quandt (ref 16) this occurs at a liquid loading of less than 450 mg of water per second and per cm of conduit periphery. In ref 15 a limit of about 100 mg/cm, s has been observed, also for water. A limit of 200 mg/cm, s is plotted into Figure 2. 1, calculated for the 16 mm internal diameter of tube of the test loop.

This reluctance of the liquid to spread on the conduit wall is of importance when designing a wall flow sampler, and also for the transport velocity for wall-attached oil.

In an investigation on oil mist lubrication, Muno (ref 14) has measured deposition and resuspension in a conduit. The oil, injected in the air line by means of a lubricator, was first deposited, but further down the conduit became almost completely air-borne again (Figure 2.2). The conditions for this observation are also shown in Figure 2.1 (marked ---).

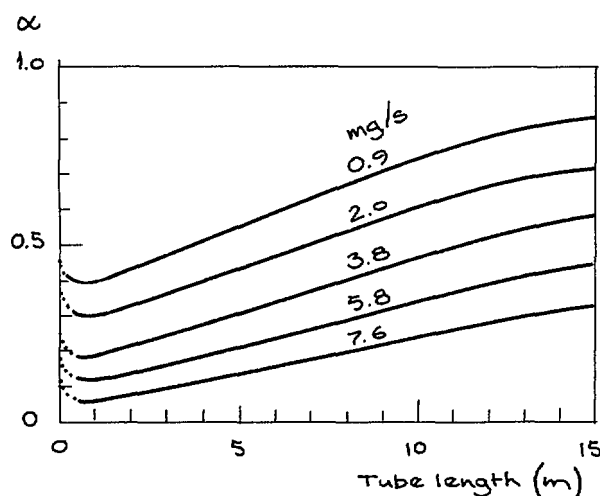
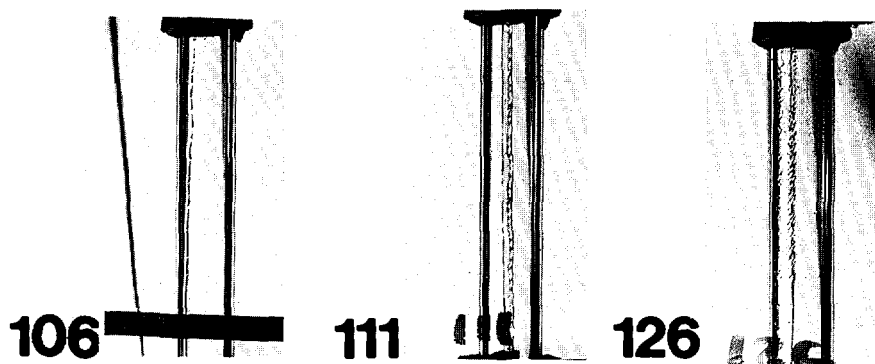


Fig 2.2 Resuspension of oil in a compressed air line. The oil is first deposited, but further down the line is partly resuspended.
 α = core oil flow/total oil flow.
 Steel tube, internal diameter 8 mm.
 Air flow $20 \text{ m}^3 \text{ (Norm)/h.}$ (ref 14).

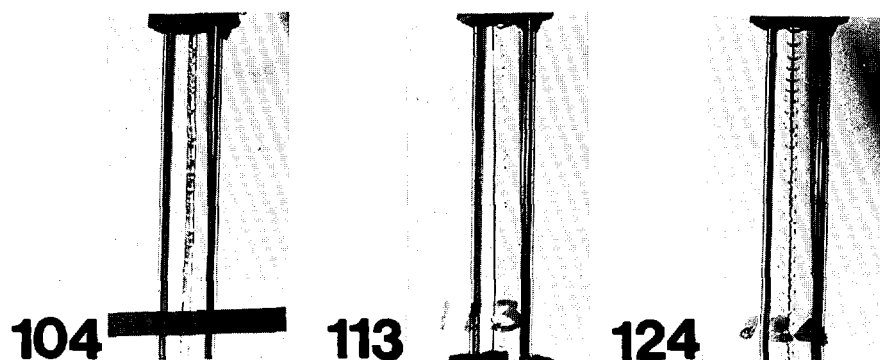
To further clarify the mode of flow at low liquid-to-gas ratios, some experiments were made in the test rig. The samplers in Figure 1.1 were replaced with a piece of glass tubing so that the flowing liquid could be observed. Figure 2.3 shows some photographs of the flow modes and also gives details on air and oil flow.

From the photographs it is clear that the oil does not form a continuous film inside the glass tube. Instead, the liquid forms a narrow rivulet, occupying only a small fraction of the conduit periphery. The same phenomenon of contraction has been observed at the sample transport tubes, Figure 3.2. It is queer to note that an increased air

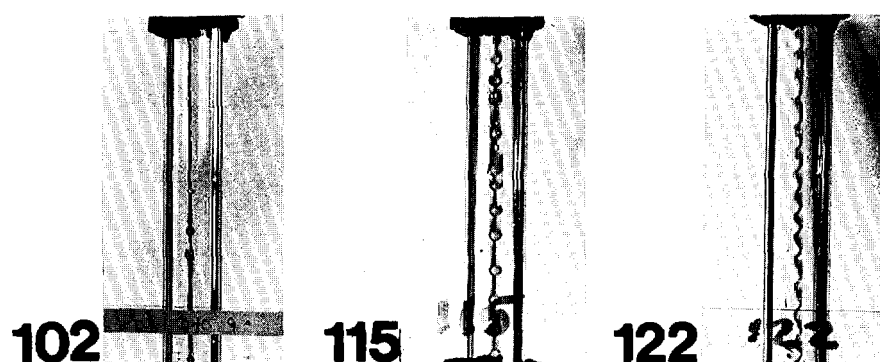
8.3 l (Norm)/s



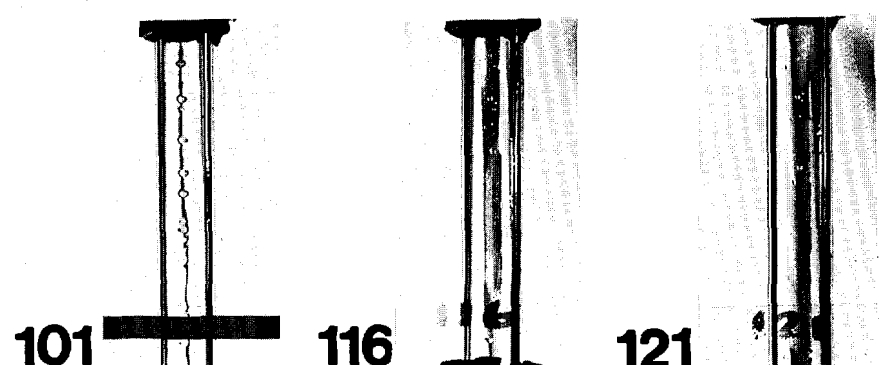
5.6 - " -



2.8 - " -



1.4 - " -



2 mg/s

3.4 mg/s

8.7 mg/s

Fig 2.3 Observed flow patterns of oil rivulet in test loop glass section. The air and oil stream vertically downwards. Atmospheric pressure.

stream makes the rivulet thinner, except at the highest liquid flow, where it instead becomes broader and tends to spread. The oil flow of 8.7 mg/s corresponds to about 2 mg per second and cm of periphery. As mentioned above, a continuous water film will develop only above c 200 mg per sec and cm of periphery.

The air and oil flows corresponding to the photographs in Figure 2.3 have been plotted in the Baker diagram. Figure 2.1 (numbers 101 - 126). The pictures support the prediction of the Baker diagram, that at high flows of air and liquid, ripples and waves are created and some liquid is torn loose forming an air-borne mist (dispersed flow). Also Muno noted high air-borne fractions at these air and oil flows. As will be seen below (p 15), the tests of the wall flow sampler also indicated a higher air-borne fraction above an air loading of 10 kg/s, m².

The information on two-phase flow of low liquid contents cited above can be summarized thus:

At the air and liquid loadings of interest to this project the liquid is completely wall-attached at low air flows and may be almost completely air-borne at high air flows. The fraction of air-borne depends strongly on the length of conduit through which the liquid has travelled. When wall-attached, the liquid moves in one or several rivulets. At the lowest air flow the liquid may be stratified in horizontal tubes, but at higher has flows conduit orientation is of little importance.

The fraction of air-borne depends on the liquid loading, but evidence is contradictory. Figure 2.2 shows a decreased air-borne fraction for more liquid, but the photographs 106, 111 and 126 of Figure 2.3 to higher resuspension at a higher liquid flow. In Figure 2.1 these photographs and the Muno experiments cover about the same area.

2.3 Wall flow sampler

Design

Some different arrangements to extract wall-attached flow are shown in Figure 2.4. The porous wall models are easy to build. A gas stream is maintained into the annular chamber from the flow core. This stream sweeps the wall flow through the porous wall. A main difficulty with this type of sampler is to determine the necessary sweeping flow. With an oil/water mixture, problems may also arise if the oil makes the porous material hydrophobic.

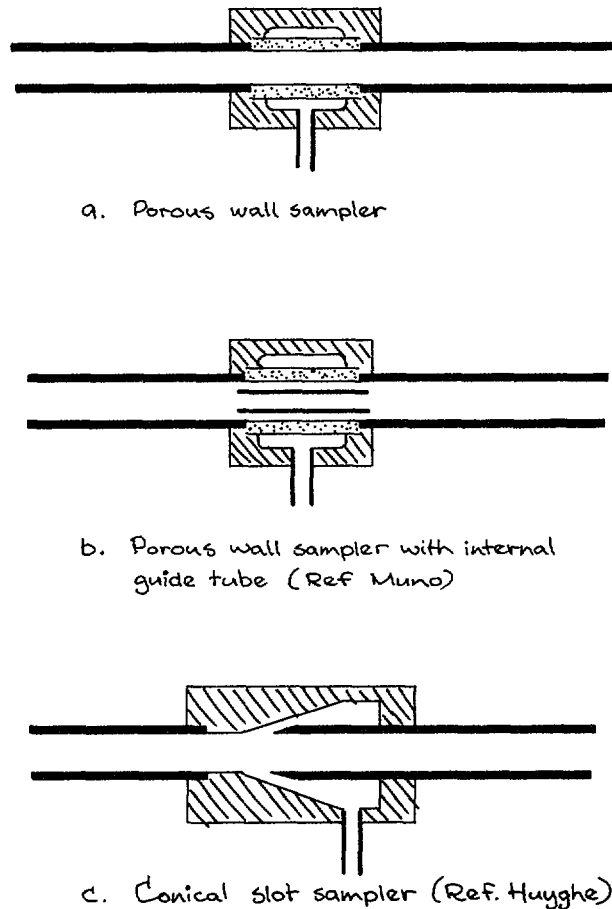


Fig 2.4 Wall flow samplers from the literature.

A sampler of the conical slot type is shown in Figure 2.4c. The liquid is conveyed into the slot by means of a concurrent air flow, and also by surface tension forces.

The kind of sampler employed in this project is shown in Figure 2.5. It is similar to the Huyghe model, except that the tube diameter is slightly smaller downstream of the slot than upstream. This simplifies manufacture, in that the centering of the upstream and downstream tubes is then not so very critical. (It has been observed that upstream tube "hangover" causes liquid to skip the slot.)

There is no theoretical foundation for the design of the wall flow sampler. Several opposing requirements must be met: a wide slot to accommodate large rivulets of liquid, but a narrow slot to get a high gas velocity into the slot; a high sampling gas flow, also to increase the slot gas velocity, but a low gas flow to minimize interference from liquid and vapours in the core flow.

The sampler is thus designed on rather weak foundations. Some experiments to test its performance were deemed to be necessary.

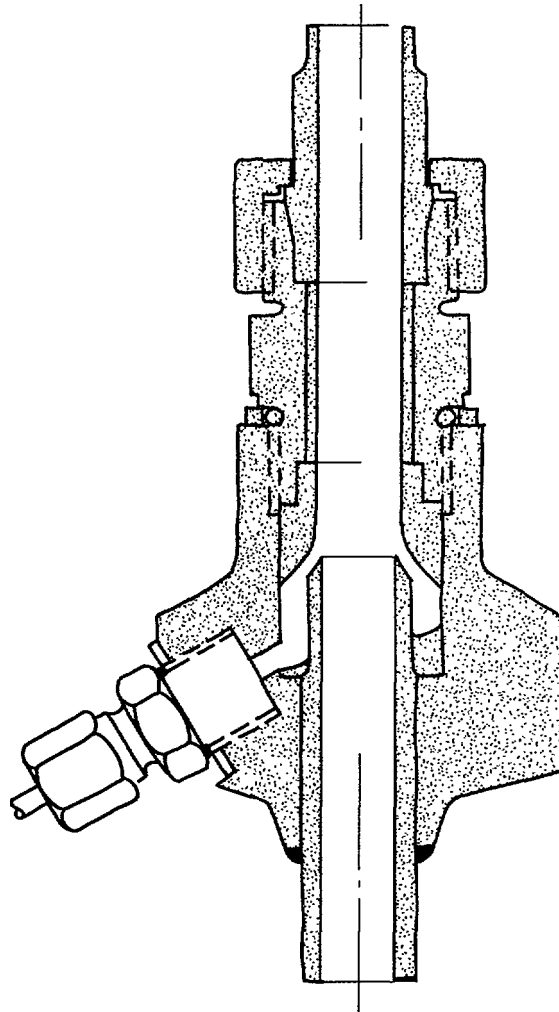


Fig 2.5 Wall flow sampler employed in the experiments.

Experiments on wall flow sampler

The sampler was mounted in the vertical section of the test loop, the flow being downwards for air and liquid. The pressure in the loop, relative to the atmosphere, was 600 kPa.

A flow of liquid was injected in the horizontal part of the test loop. Care was taken to place the liquid on the tube wall, avoiding the formation of droplets in the air stream.

Liquid extracted by the wall flow sampler was collected in a cylinder at A, Figure 2.6. Liquid passing the sampler was collected at B.

The liquid flows were calculated as collected volumes divided by sampling time. For injected flow a special flow-meter was used.

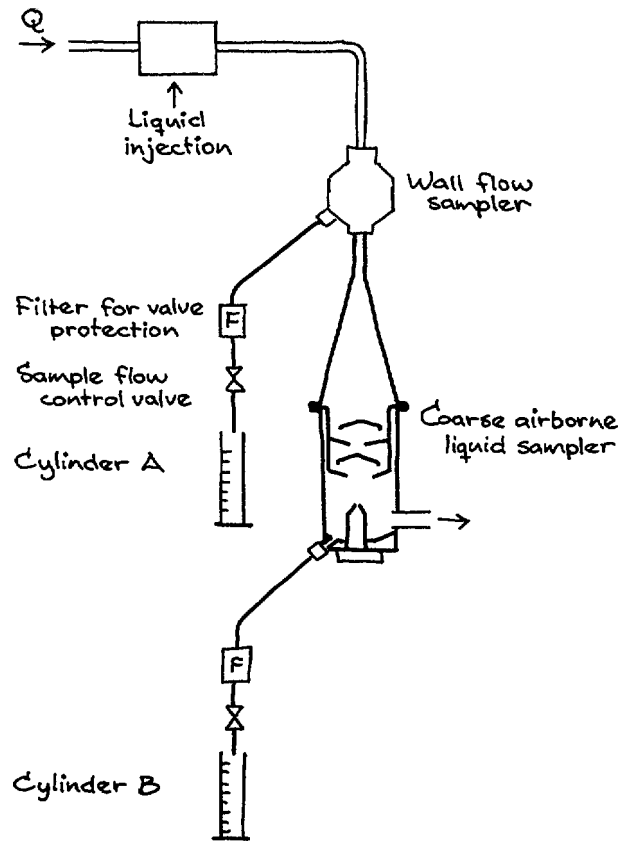


Fig 2.6 Experimental arrangements for tests of wall flow sampler.

Sampling efficiency η is calculated as the ratio between the obtained sample flow q_A and the total flow $q_A + q_B$

$$\eta = \frac{q_A}{q_A + q_B}$$

The liquid flows employed are equal to or exceed the flows corresponding to the upper limit of concentration, $1\,000\text{ mg/m}^3$ (Norm). It is felt that this should suffice for the whole concentration range, since a lower flow should be easier to deflect into the sampling slot.

Experiments with water

Observed efficiency at the slot width 0.3 mm is shown in Figure 2.7 as a function of extracted air flow. Efficiency increases with increasing air flow, but complete collection cannot be achieved at this slot width.

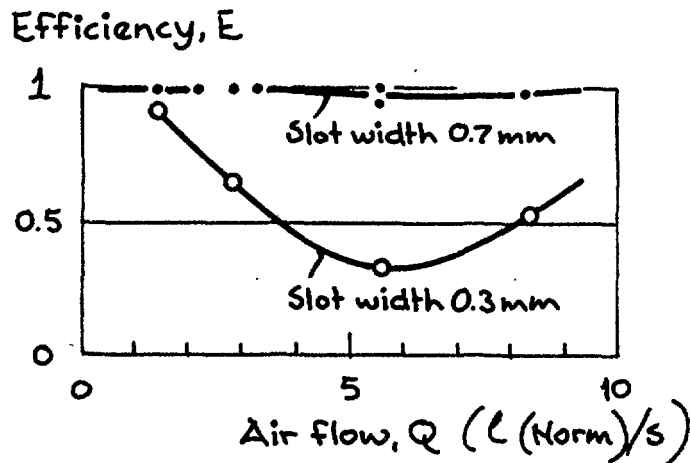


Fig 2.7 Wall flow sampler efficiency at different slot widths and air flows.

With the slot width increased to 0.7 mm the efficiency rose to almost 100 % at all sample gas flows. Only small amounts of liquid were found at B.

This result also shows that, under the circumstances of the experiment, there was no liquid in the core flow. In the tests with the slot width 0.3 mm the flow conditions were the same, and the liquid found at B was thus wall flow, which had skipped the sampler.

The investigated range of air and liquid flows is plotted in Figure 2.1 (marked o - o - o).

Experiments with oil

Oil of type 0 was used. The experimental arrangements were the same as with water, but only one slot width, 0.7 mm, was tested.

The tests showed that with a high air flow in the conduit the injected oil (about 8 mg/s) could not be extracted completely, Table 2:1.

TABLE 2:1 INFLUENCE OF SAMPLE AIR FLOW ON WALL
FLOW SAMPLER EFFICIENCY

Main air flow l (Norm)/s	Sample air flow ml (Norm)/s	Extracted through wall flow sampler %
2.8	100	100
2.8	200	99
2.8	385	99
5.6	100	69
5.6	200	75
5.6	385	67
8.3	100	66
8.3	200	67
8.3	385	66

The extracted gas flow, intended to carry the wall-attached liquid into the slot and through the sampling line, was varied. The table above shows that this did not influence the amount of oil collected. It is concluded that the oil, as opposed to water, is partly in an air-borne state, not accessible for sampling as a wall flow.

This series of tests corresponds to the photographs 121 - 124 of Figure 2.3. The investigated range of air and liquid flows is also shown in Figure 2.1 (marked o - o - o).

2.4 Coarse air-borne liquid sampler

This sampler is intended for collection of coarse air-borne material that cannot be sampled by the Levin nozzle (p 21). This fraction has a strong tendency to become deposited. If the sampler were not there, this liquid would soon be deposited anyway and take part in the exchange of material between wall flow and core flow. Because of this, the sample could be said to be a part of the wall flow. On the other hand, it has a higher velocity of transport and is in this way more similar to the fine air-borne mist.

This sampler could also be used to collect the wall flow if there is no interest in the subdivision of these fractions.

Design

The sampler works through the combined action of inertia forces and gravitation. The outlines are shown in Figure 2.8.

The unit is intended to operate with the gas and liquid flowing vertically downwards. At high gas flows, coarse particles are impacted on the surfaces below the nozzles; at low gas flows sedimentation will deposit the larger particles.

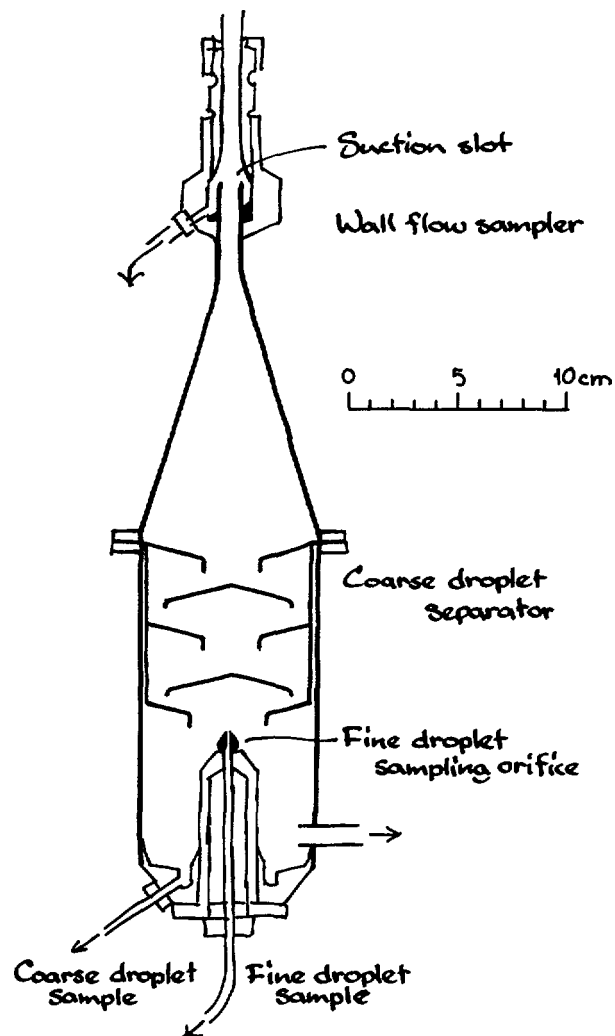


Fig 2.8 Sedimentation-impaction sampler for coarse air-borne liquid.

Impaction

Impaction efficiency can be calculated from published data, (ref 13, p 229). This kind of deposition is governed by the Stokes number:

$$\text{Stk} = \frac{v_o d_p^2 \gamma_p}{9\eta D}$$

where

- v_o velocity in the nozzle (m/s)
- d_p particle diameter (m)
- γ_p particle density (kg/m^3)
- η gas viscosity (Ns/m^2)
- D nozzle diameter (m)

About 50 % of the particles of the size in question will be deposited at a Stokes number of 0.2. If the Stokes number becomes lower, the deposition efficiency will be smaller, and vice versa. The impaction efficiency for the nozzles in Figure 2.8 has been calculated, Figure 2.9.

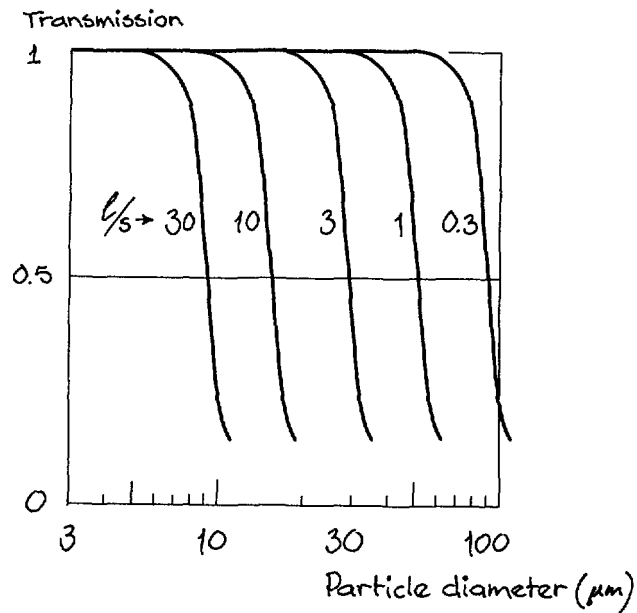


Fig 2.9 Calculated transmission through the sedimentation-impaction unit, based on the impaction effect. Air flow 0.3 - 30 l (Norm)/s. Absolute air pressure 700 kPa.

Sedimentation

At low air flows sedimentation replaces impaction. To calculate the deposition effect, the sedimentation-impaction unit is imagined to consist of six consecutive boxes, Figure 2.10. We assume for a moment that all particles are of the same size. If the aerosol in each box is well mixed, the rate of deposition in a box is

$$c_i A_i v_s \text{ (kg/s)}$$

The notation is explained in the figure. The mass balance for a box becomes

$$Q' c_{i-1} = c_i A_i v_s + Q' c_i$$

and for all boxes

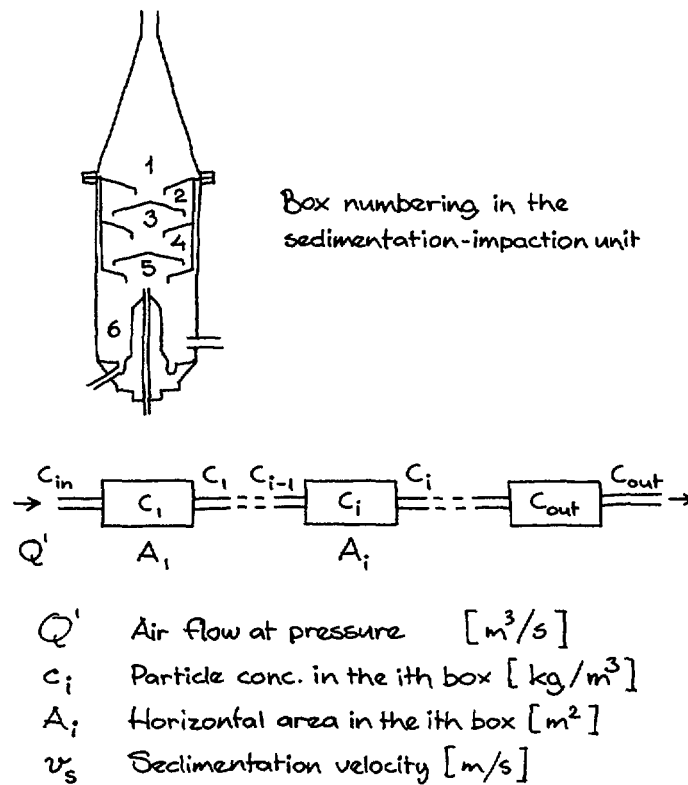


Fig 2.10 Sedimentation-impaction unit. Sedimentation in a number of series-connected boxes.

$$\frac{c_{out}}{c_{in}} = \prod \frac{Q'}{Q' + A_i v_s}$$

For the geometry in question, we can assume all A_i to be about the same. With six boxes, the concentration reduction becomes

$$\frac{c_{out}}{c_{in}} = \left(1 + \frac{A v_s}{Q'}\right)^{-6}$$

The expression has been evaluated for a number of air flows, Figure 2.11. By varying the particle diameter the transmission through the unit is obtained for all sizes.

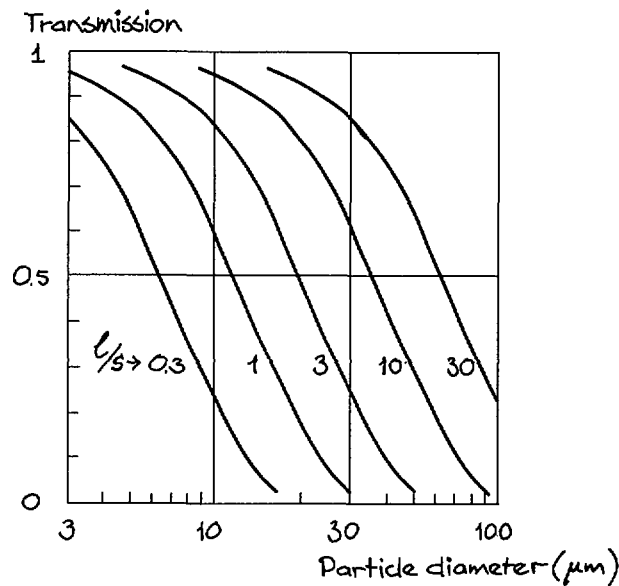


Fig 2.11 Calculated transmission due to the sedimentation effect. Air flow 0.3 - 30 l (Norm)/s. Absolute air pressure 700 kPa.

Total deposition

It now remains to combine the deposition effects of gravity and inertia. This cannot be done on theoretical grounds, but a qualitative picture is easily drawn, Figure 2.12.

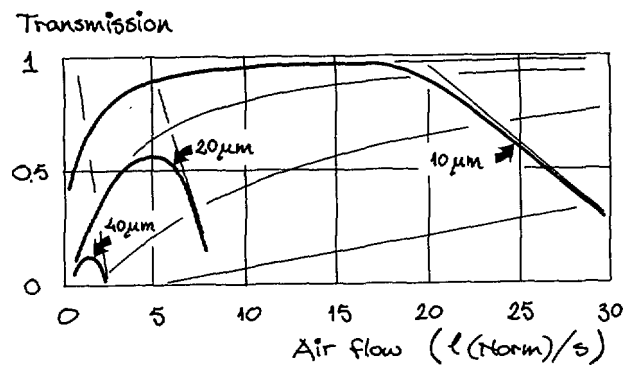


Fig 2.12 Estimated transmission for particles through the sedimentation-impaction unit, gravity and inertia working simultaneously. Absolute air pressure 700 kPa.

The penetration of particles varies with the flow. 10 μm particles are transmitted at all flows but the lowest, while only a small fraction of the particles greater than 40 μm will pass at any flow.

Tests

The design described above has not been practically tested. A similar sampler has been used in the tests with the wall flow sampler to collect passing liquid (Figure 2.6).

2.5 Gas and fine air-borne liquid sampler

Design

The usual way to withdraw a particulate sample from a streaming aerosol is to arrange an isokinetic probe. This is a nozzle with its thin-walled opening directed against the flow, and with a velocity in the inlet equal to the velocity in the main stream. This requires that the sampling flow is proportional to the main flow, and under varying flow conditions this is not easily achieved.

Instead it is advantageous to use a special kind of sampler, here called Levin sampler (ref 11). Here the aerosol is extracted through a small orifice at a high velocity. The high pressure available makes this easy. The jet of air from the nozzle leads to high deposition in

the sampling line, but this is not so serious with a liquid as with solid particles. Deposition takes place anyway in the filter protecting the flow-controlling valve in the sample transport line.

The sampler extracts a predictable fraction of particles of a given size, the fraction being expressed by

$$\mu = 1 - 0.8 K + 0.008 K^2 - \dots$$

$$K = \tau (4\pi/q')^{1/2} U^{3/2}$$

where

- μ sampling efficiency = (conc in sample)/conc in main stream (-)
- $\tau = d_p^2 \rho_p / 18\eta$ particle relaxation time (s)
- d_p particle diameter (m)
- ρ_p particle density (kg/m^3)
- η gas viscosity (Ns/m^2)
- q' sample flow (m^3/s)
- U vectorial sum of gas velocity and sedimentation velocity (m/s)

The formula is applicable only at efficiencies greater than 0.8.

The velocity of the oncoming particles, U , is made low by using a wide exit opening of the coarse droplet separator (Fig 2.8).

Sampling efficiency has been calculated at a sample flow of 100 ml (Norm)/s, Figure 2.13. When the air flow is high, only small particles are sampled correctly, but this is of no importance, since the sedimentation-impaction unit effectively removes any large particles at high flows.

Tests

A Levin sampler has been built and tested in the test loop. Unfortunately the amount of liquid streaming into the sampler was too small for sample transport. As is explained in some detail in Chapter 3 (Sample transport), the liquid does not move in a sample transport line if the amount of liquid is too small. The maximum liquid flow from the Levin sampler will be

$$1\,000\text{ mg/m}^3 (\text{Norm}) \cdot 100\text{ ml (Norm)/s} = 0.1\text{ mg/s}$$

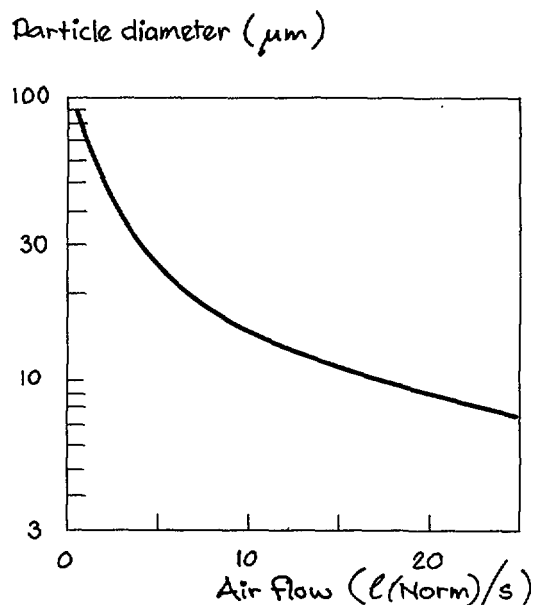


Fig 2.13 Largest particles to be sampled with an error less than 0.8 in the fine core flow sampler. Absolute air pressure 700 kPa.

The flow is then normally less than the minimum acceptable flow of 0.1 mg/s (Figure 3.1).

Under the given conditions, collected liquid cannot move in the sample transport line. But on the other hand, with a low concentration of liquid, the liquid can be evaporated and moved in the gas phase. It has been calculated that, under reasonable assumptions regarding the oil, a temperature of about 250°C would suffice to get a vapour pressure corresponding to 1 000 mg/m³ (Norm). Thus a heated sampling line can solve this problem. No experiments have been done on this.

2.6 Conclusions concerning samplers

Wall flow sampler

About 50 tests on the wall flow sampler have been recorded. It is believed that the unit is effective. But as the design is empirical, the basis for scaling to other pipe diameters is uncertain.

Corse air-borne liquid sampler

The sedimentation-impaction unit has only a theoretical foundation, and no practical tests have been made. From experience, sedimentation and impaction effects can be predicted with some confidence.

Vapour and fine air-borne liquid sampler

Also this sampler is a theoretical design, and only qualitative experiments have been carried out. Further tests are advisable.

2.7 Calculation of vapour and liquid flows from sample flows

To calculate the transport of vapour and liquid in the compressed air line from the sample flows, the following formulas apply approximately:

$$\varphi(\text{wall}) = q [c(\text{wall}) - c(\text{core, fine})]$$

$$\varphi(\text{core, coarse}) = q [c(\text{core, coarse}) - c(\text{core, fine})]$$

$$\varphi(\text{core, fine}) = Q \cdot c(\text{core, fine})$$

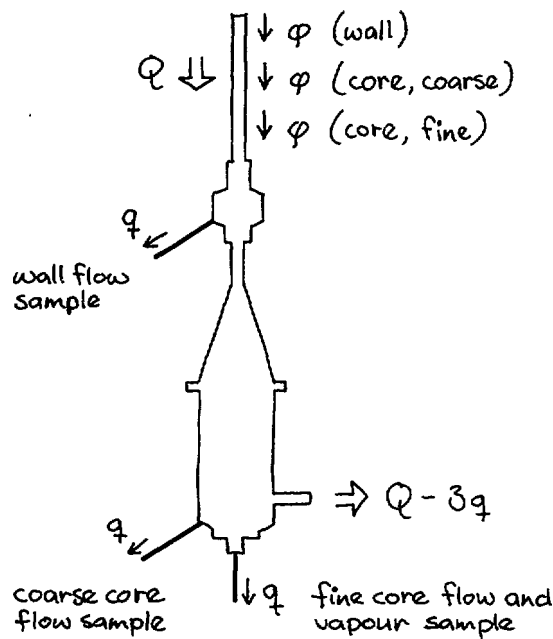
The notation is explained in Figure 2.14. All concentrations and flows are referred to standard conditions (Norm = 101325 Pa, 20°C). The formulas apply to oil as well as water. The concentrations c are supposed to be indicated on the instruments, chapter 5.

3. SAMPLE TRANSPORT

From the sampling points on the compressed air line, a mixture of air and liquid is conducted to the measuring instruments. In the present investigation, teflon tubing of 1.7 mm internal diameter was used. Pressure reduction to a near atmospheric level takes place in a needle valve, protected by a sintered metal filter. The flow from the needle valves is directed along more teflon tubing to different instruments by means of ball valves.

These components for sample transport determine the time of response for the measuring system. The time of response t_t is given by:

$$t_t = m_t / \dot{m}$$



- ϕ contaminant mass flow (kg/s)
 Q main stream air flow (m^3 (Norm)/s)
 q sample air flow (m^3 (Norm)/s)
 c (core, fine) small particle and vapour mass concentration in main stream and sample stream (kg/m^3 (Norm))

Fig 2.14 Notation for calculation of contaminant flows.

where

m_t = the amount of liquid accumulated on the interior surfaces of the sampling system

\dot{m} = mass flow of the liquid

It can be assumed that only a minor part of the liquid is transported as air-borne droplets. Due to rivulet formation, and the amount of liquid in the sintered filter and in joints and other crevices of the manifold, it is difficult to predict how much liquid will accumulate in the transport system.

3.1 Estimation of transport velocity

A crude estimate of the transport velocity for low flows of liquid can be made if one assumes a laminar liquid film on the wall of the sample conduit. The shear stress from the streaming air is transmitted through the film to the solid tube wall. The stress is (ref 17, p 553), with thin films:

$$\tau_o = \frac{D}{4} \frac{dp}{dx}$$

where

- τ_o shear stress in the film on the wall (N/m^2)
- D conduit diameter (m)
- p air pressure (N/m^2)
- x coordinate along conduit axis (m)

The pressure drop along the conduit, dp/dx , can be expressed by the friction factor λ

$$\tau_o = \frac{\gamma_g \lambda \bar{u}^2}{8}$$

where

- γ_g air density (kg/m^3)
- \bar{u} mean air velocity (m/s)

There are several ways to obtain the friction factor, e.g. the Blasius equation

$$\lambda = \frac{0.3164}{(Re(air))^{\frac{1}{4}}}$$

where

$$Re = \frac{\bar{u} \gamma_g D}{\eta}$$

- η air viscosity (Ns/m^2)

With the liquid film moving in a laminar flow over the tube wall, the velocity is zero at the wall. At the interface air-liquid the liquid velocity is largest.

$$v_{\max} = \frac{\tau_o}{\eta_{\text{liq}}} \cdot a$$

and, for a thin film

$$v_{\text{mean}} = v_{\max}/2$$

a is the film thickness, which depends on the mass flow:

$$\dot{m}_{\text{liq}} = \rho_{\text{liq}} v_{\text{mean}} \pi D a$$

Eliminating the film thickness, one gets

$$v_{\text{mean}} = \sqrt{\frac{\tau_o \dot{m}_{\text{liq}}}{\rho_{\text{liq}} \eta_{\text{liq}} 2\pi D}}$$

From this expression the transport velocity in sampling lines can be calculated. Figure 3.1 shows some results obtained for oil. Below 1 mg of oil per second the oil film is expected to move at a velocity of less than 1 mm/s.

3.2 Experiment on transport velocity

In practical experiments on transport velocity the liquid was observed to move about five times faster than predicted by the laminar film theory. As could be seen through the teflon tube wall, this situation arises because the liquid is not evenly distributed around the tube periphery, but restricted to a narrow rivulet, Figure 3.2. This is a phenomenon of the same kind as described in connection with the samplers, p 8. It is probably not a non-wetting effect of oil-on-teflon, because the velocity of oil in steel tubing is also about five times higher than theoretically predicted. The steel is easily wetted by oil.

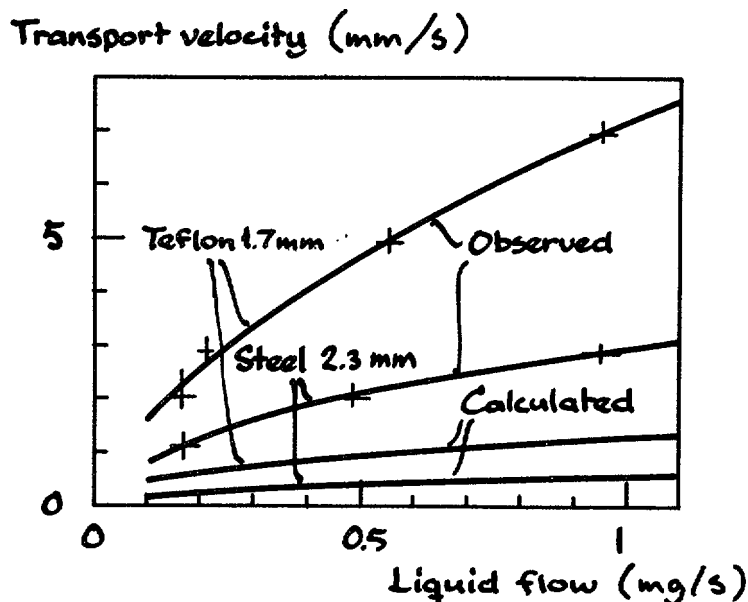


Fig 3.1 Observed and calculated transport velocity for oil in sampling lines. Oil viscosity 0.1 Ns/m^2 , gauge pressure 600 kPa, gas flow 100 ml (Norm)/s.

The velocity in tubes is only part of the answer to the question of response time. The total response time during an experiment with the test loop turned out to be 12 minutes. In this case the oil was injected into the sample line at the wall flow collector ($\dot{m} = 0.5 \text{ mg/s}$) and observed at the flame ionization detector. The sample transport circuit included about 2 m of tubing, one sintered metal filter, two valves and the evaporation-condensation unit, containing approximately 2 m of heated steel tubing.

4. SAMPLE PREPARATION

4.1 Requirements regarding sample flow to instruments

The sample stream consisting of a mixture of air, water, and oil is not immediately suitable for admission to measuring instruments. Thus for the determination of water and water vapour it is first necessary for the oil to be removed.

It is also necessary to shunt the sample flow of 100 ml/s. The electronic humidity meter requires a flow of about 10 ml/s, and the hydrocarbon analyzer about 1 ml/s. Achievement of this sub-sampling has

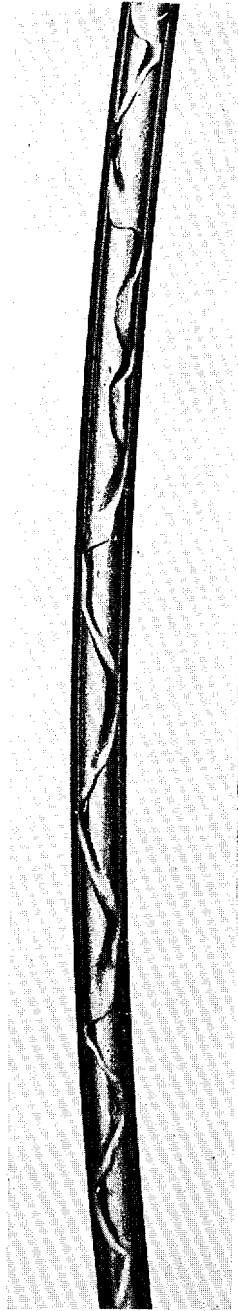


Fig 3.2 Rivulet of oil in a teflon sampling line.

entailed some effort. An evaporation-condensation technique was eventually adopted.

It was found necessary to dilute the samples in order to come within the measuring range of the instruments.

4.2 Mechanical homogenization of sample flow

Shunting of the sample stream implies the same difficulties as sampling of the main stream discussed earlier. In an attempt to form a more homogeneous mixture of air and liquid, the sample stream was forced through an ultrasonic nozzle. Figure 4.1 shows the experimental arrangements.

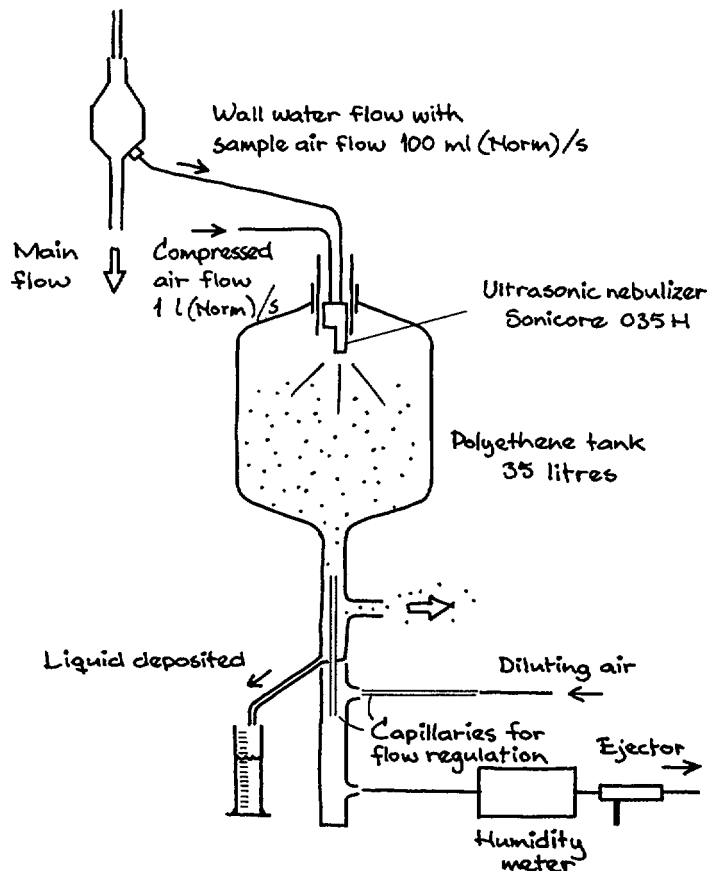


Fig 4.1 Experiment on sample homogenization by means of ultrasonic nebulizer.

The primary size of the ultrasonic nozzle was below $10\text{ }\mu\text{m}$. Although the total air flow was increased to 1 l(Norm)/s , the concentration of air-borne liquid in the tank could reach $30\text{ }000\text{ mg/m}^3$ at maximum flow of liquid in the test loop. At such concentrations droplet growth through coalescence is fast, and the enlarged droplets are deposited to an appreciable extent.

A subsample withdrawn from the tank would thus not be representative of the total liquid flow, especially if deposition was selective with respect to oil or water. The spray tank was not a good solution to the subsampling problem.

4.3 Sample vaporization

Some experiments on the vaporization of the liquid have been made to investigate the possibility of subsampling in the gas phase. The conditions for evaporation of water are well known, but the oil has merited a special examination.

The medium viscosity lubricant fraction of mineral oils has 25 - 35 carbon atoms per molecule. The oil, being a mixture of very many hydrocarbon compounds, has no defined boiling point. The range of vapour pressures covered by the oil components is shown in principle in Figure 4.2. When the oil is heated to 350 - 400°C, most of the oil compounds reach a pressure sufficient for fairly rapid evaporation, even if the liquid does not boil.

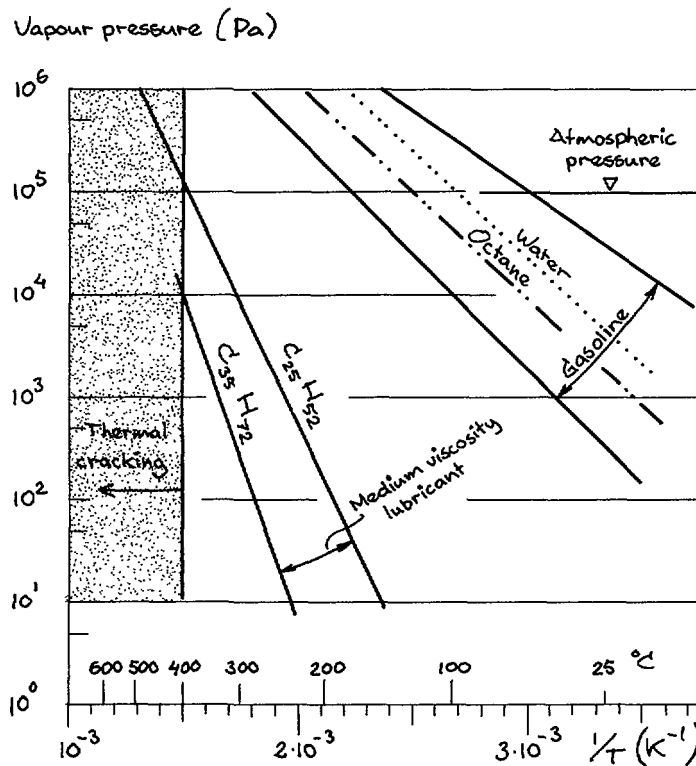


Fig 4.2 Approximate vapour pressure for medium viscosity lubricating oil.

When oil is heated above 350 - 400°C, some less desirable effects might also occur, namely cracking, polymerization, oxidation and coke formation.

Hydrocarbon cracking gives smaller molecules and the process is used for transforming oil to gasoline and gas. The process is thus advantageous for the purpose of oil evaporation and sample subdivision.

Together with the break-up of molecules, there is also a polymerization process, leading to hydrocarbons of higher viscosity. These semi-solid substances might be deposited in the evaporator and must be avoided. The same applies to the solid coke.

Using the cracking as a measure of the chemical reaction taking place on heating, we can express the reaction velocity as

$$A = A_0 e^{-kt}$$

where

A amount of material not yet reacted (kg)

A₀ starting amount of material (kg)

The reaction velocity time constant k is obtained through the Arrhenius equation

$$k = be^{-\frac{E_A}{RT}}$$

where

E_A heat of activation (J/mol)

R gas constant, 8.31 (J/mol K)

T absolute temperature (K)

For a light petroleum fraction, gas oil, it has been observed (ref 7, p 35)

$$E_A = 200 \text{ kJ/mol}$$

$$b = 3.22 \cdot 10^{12} \text{ 1/s}$$

In order to achieve evaporation of the oil with smallest possible cracking, polymerization and coking, the time at high temperature should be as short as possible. Figure 4.3 shows the calculated conversion at short retention times. Under the assumed conditions, a surface temperature up to 450°C can be allowed in the evaporator.

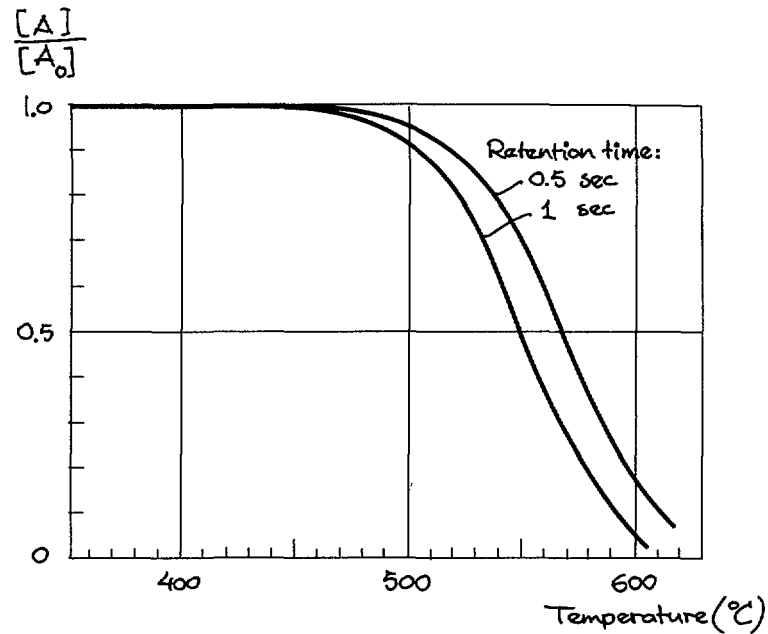


Fig 4.3 Temperature and time influence on hydrocarbon cracking

$$\frac{A}{A_0} = e^{-kt}$$

$$k = b \cdot e^{-\frac{E_A}{RT}}$$

$$E_A = 2 \cdot 10^5 \text{ (J/mol)}$$

$$R = 8.31 \text{ (J/mol)}$$

$$T = 273 + \text{temp (}^\circ\text{C)}$$

$$t = \text{time (s)}$$

Technical oils vary considerably in composition, and Figures 4.2 and 4.3 are only intended to give an indication of the temperatures and times involved. But it seems clear that many oils can be vaporized without destruction.

Increased temperature also leads to oxidation of the oil. It has not been possible to evaluate the importance of this factor. Some later references are 1, 4, 18.

4.4 Evaporator

As concluded in the previous paragraph, the oil-water-air mixture from the sampling point should be heated as fast as possible. As the oil partly flows on the evaporator walls, the wall temperature must not exceed the desired final air temperature very much. Instead the heat transmitting area must be made large.

The design chosen is shown in Figure 4.4. A helical coil of stainless steel tubing is wound on a cast iron core and heated in a cylindrical oven. The tubing has an internal diameter of 2.3 mm and a length of 2 m. A thermocouple measures the steel tubing temperature close to the outlet. A second thermocouple in the oven is used for automatic temperature regulation.

In the working range of interest and at 100 ml (Norm)/s, the gas temperature at the outlet is c 30°C below wall temperature.

To investigate the risk of deposit formation in the evaporator, an experiment was carried out with a simpler evaporator, containing only 0.5 m of tubing. At an air flow of 100 ml (Norm)/s and oil 0 the amount of injected oil which did not evaporate but dripped out as liquid was observed to be:

Wall temperature	Approx air temperature	Not evaporated
°C	°C	%
305	215	4.5
350	260	3.2
395	305	1.9

Each temperature was maintained for 6 hours. The pressure drop over the unit was observed to be constant at the two lower temperatures, but at 395°C the pressure drop increased during the course of the experiment. This implies that in this case a deposit was formed in the heating coil.

For work with the larger evaporator, it was decided to use the wall temperature 325°C, giving an air temperature of 295°C. The amount not evaporated should then be insignificant, and the risk of deposits small.

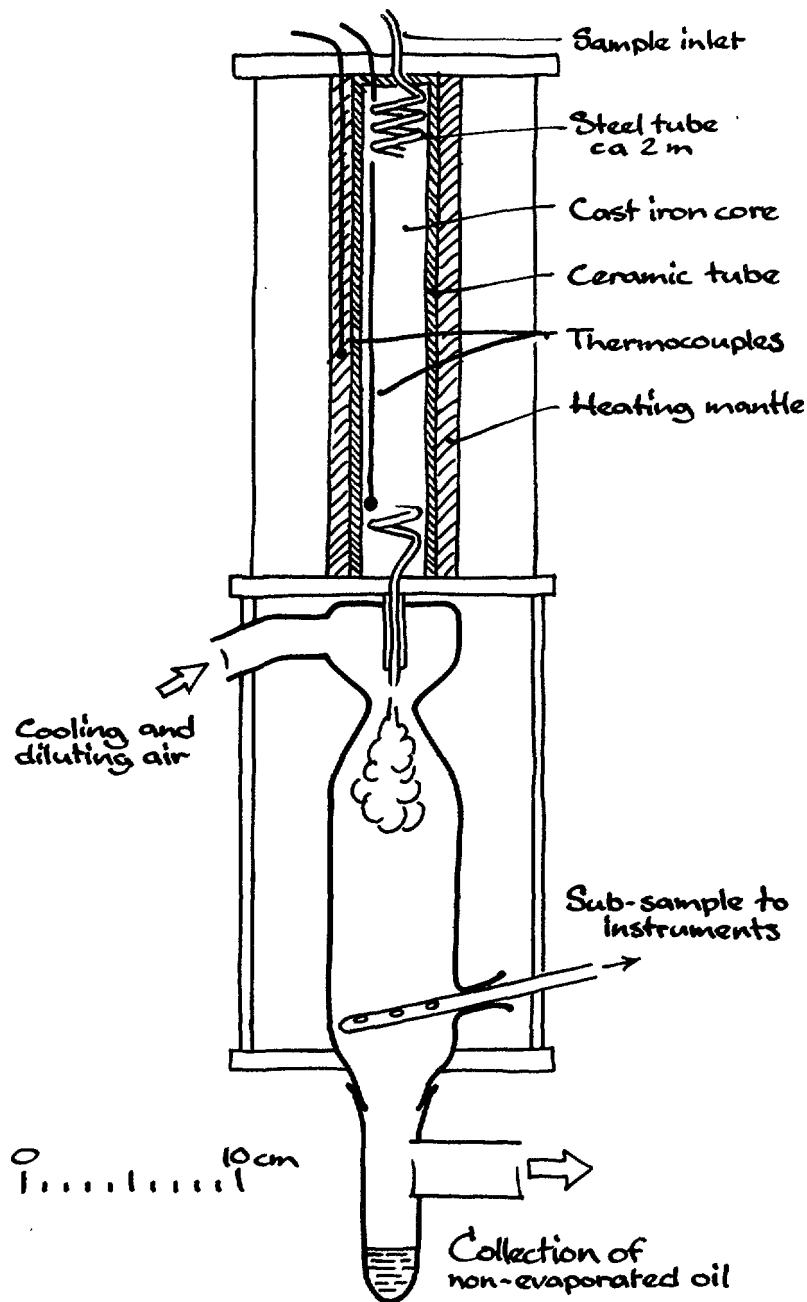


Fig 4.4 Evaporation-condensation unit for sub-sampling of samples obtained at compressed air line.

4.5 Condensation unit

Sample conditioning for oil measurement

Oil cannot remain in the vapour phase at the relatively low temperature required by the flame ionization detector. When measuring oil,

therefore, the temperature was reduced by mixing cool air with the hot sample stream from the evaporator. This caused the oil vapour to condense, forming an aerosol of very small particles. Such an aerosol is easily sampled. Figure 4.4 shows the form taken by the evaporation-condensation unit in practice.

Apart from cooling the effluent gas from the evaporation unit, the admixed air also dilutes the oil-air mixture. This is necessary to get within the measuring range of the flame ionization detector.

Sample conditioning for humidity measurement

A stream of compressed air, free of oil and liquid water, is easily sampled. If it is not very dry (dew point above -20°C at atmospheric pressure), the water vapour content is also readily measured. Determination of the humidity in air of lower dew point demands considerable care if errors, due to water diffusing from or through sampling line walls, are to be avoided.

If there is liquid in the compressed air, it must be incorporated in the sample. Any oil present may contain adsorbed or emulsified water. Lubricants for compressed air tools often have emulsifying additives. While it is important for this water to be released, oil must at the same time be prevented from reaching the humidity meter.

With a temperature of about 100°C in the evaporation-condensation unit, most water present will be vaporized, while most of the oil will remain in the liquid phase. The addition of air for purposes of cooling and dilution can be done in the condensation section, thus complying with the requirement for keeping the dew point below the highest concentration accepted by the humidity meter.

The air is then sampled and filtered to remove any oil droplets present. It is essential that the temperature at the filter is lower than at the humidity meter, so as to prevent oil condensation in the meter.

This system does not permit the measurement of humidity in very dry air. The evaporator, the condensation unit and the filter offer large areas for deposition and desorption of water vapour, and the time of response becomes too large for practical purposes.

In this case the evaporation-condensation unit has to be by-passed and the sample fed directly to the humidity meter.

5. INSTRUMENTS

5.1 Investigated methods

It has been one of the aims of this project to find instruments suitable for making continuous measurements without recourse to manual methods and laboratory facilities. These instruments were required to be portable and simple to use.

For humidity measurements, there is a wide choice of instruments, which are moreover in continuous use in industry. An instrument of this class was obtained and tested.

Adsorption tubes for water vapour, with an indicator for the amount of water absorbed, were also tested. Similar tubes for other vapours are common in occupational safety work.

The standard laboratory method for the determination of small quantities of oil is the measurement of the infrared adsorption in a liquid sample. It was not thought that this method could be easily adapted to permit continuous measurements on an air-borne stream of oil. Instead a hydrocarbon analyzer of the flame ionization type was chosen. This instrument reacts to the gravimetric concentration of hydrocarbons in air.

5.2 Humidity measurement

The range of interest is $10 - 3\,000 \text{ mg/m}^3$ (Norm), but the instrument's measurement range should extend to higher humidity, which may occur when there is liquid water in the sample. The dew point meter with a cooled mirror is applicable, but it is fairly sensitive to contamination.

Instead the preference lay with another type equipped with a sensor in the form of an aluminium oxide film. The oxide film adsorbs water in proportion to the water content of the surrounding air. Electrodes, on either side of the film, measure film capacitance or resistance, then being a function of the amount of water adsorbed [ref 10].

The sensor should be protected from high relative humidity and is therefore mounted in a chamber operating at 50°C . The sample stream must be free of oil which, should it be deposited on the sensor, would block its pores. The sample stream should be about 10 ml/s .

It was found necessary to recalibrate the humidity meter at regular intervals. It is not known whether the unsatisfactory stability was a feature only of the instrument used or whether it is characteristic of these instruments generally. For calibration purposes a humid-air generator was constructed, where saturated air was mixed with very dry air in known proportions.

The humid-air generator was also used to investigate the behaviour of indicating adsorption tubes for water vapour, manufactured by Drägerwerk, Lübeck, BRD. These proved very handy to use and are specific to water vapour. But the calibration factor depends on the water vapour concentration, Fig 5.1. It thus becomes necessary to use different calibration curves for different sample volumes, Fig 5.2.

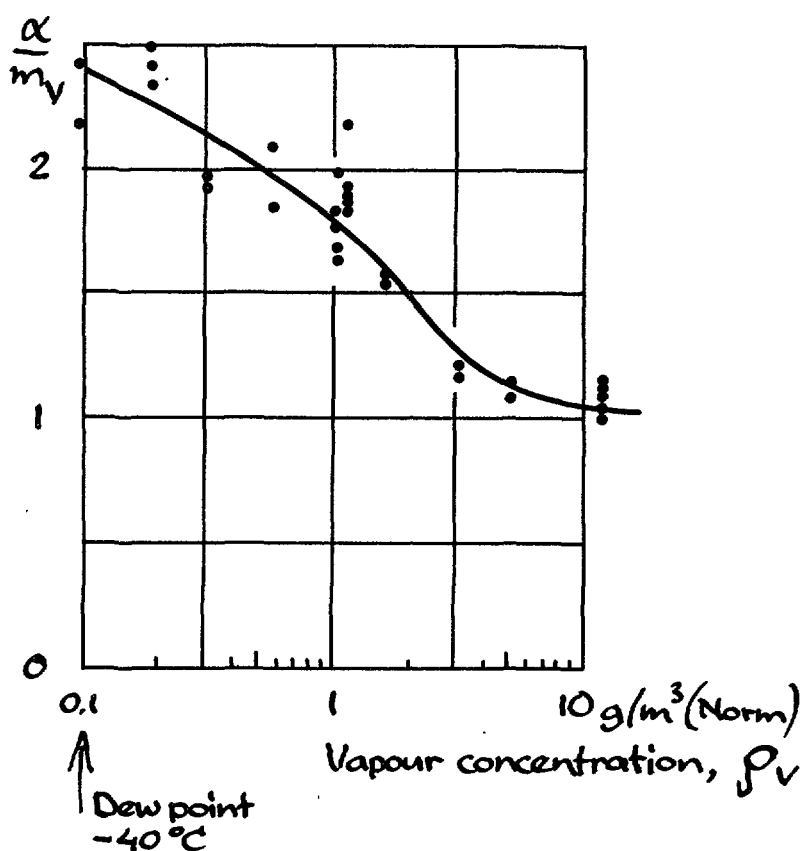


Fig 5.1 Observed ratio between indicated (α) and supplied (m_v) amount of water vapour in Dräger indicating absorption tubes. Air flow 35 ml (Norm)/s, gauge pressure at tube inlet c 20 kPa.

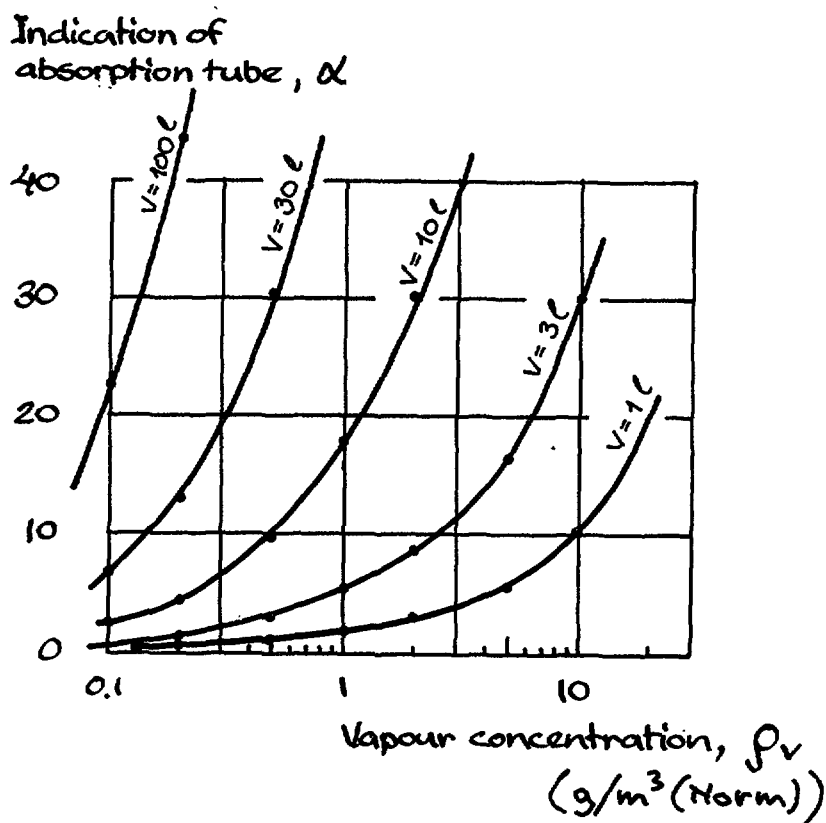


Fig 5.2 Calibration curves for water vapour in Dräger indicating absorption tubes, at different volumes of sample (V). Air flow 35 ml (Norm)/s, gauge pressure at tube inlet c 20 kPa.

5.3 Hydrocarbon measurement

The flame ionization detector responds to carbon in organic chemical compounds. It is not sensitive to carbon oxides or water vapour as long as the concentrations are not so high as to dilute the air sample.

Essentially the instrument comprises a small hydrogen-air burner, an ion collecting electrode around the burner flame, and a sensitive amplifier for the ion current. The current is directly proportional to the number of organic carbon atoms brought into the flame per unit time. The measuring range extends from 1 mg of hydrocarbon per m³ of sample to about 1 g/m³.

After having reviewed present theories on the operation of the flame ionization detector it is concluded that cracked and oxidized hydrocarbons should give a response only slightly smaller than a low-molecular hydrocarbon.

A flame ionization detector was obtained from FOA, Stockholm (The Research Institute of National Defence) [ref 5]. The FOA design has the special advantage of permitting aerosol particles to enter the flame. As was mentioned earlier, this is essential if high-boiling hydrocarbons are to be measured. The instrument requires a sample flow of precisely 1.17 ml/s, and the inlet pressure should not vary more than ± 200 Pa, gauge pressure.

A flame ionization detector was calibrated with propane to determine the relationship between ionization current and carbon concentration in the sample. It was found that

$$I_{\text{ion}} = 2.50 \cdot 10^{-5} c_{\text{C}}$$

where

I_{ion} = ionization current (A)

c_{C} = carbon concentration in sample (kg/m^3 (Norm))

When dealing with saturated hydrocarbons of high molecular weight ($\text{C}_n \text{H}_{2n+2}$, $\text{C}_n \text{H}_{2n}$, $n = 25 - 35$), such as those in lubricating oil, the above correlation can also be expressed as

$$I_{\text{ion}} = 2.14 \cdot 10^{-5} c_{\text{HC}}$$

where in that case

c_{HC} = hydrocarbon concentration in sample (kg/m^3 (Norm))

With the evaporation-condensation unit connected to the flame ionization detector as in Figure 5.3, the relation between oil mist concentration (c_{HC}) and ionization current was investigated.

A measured flow of oil was injected in a sample air stream of 100 ml (Norm)/s. Hydrocarbon concentration in the condensating chamber was calculated as

$$c_{\text{HC}} = \frac{(\text{injected oil flow}) \times (\text{oil density})}{(\text{sample air flow}) + (\text{dilution air flow})}$$

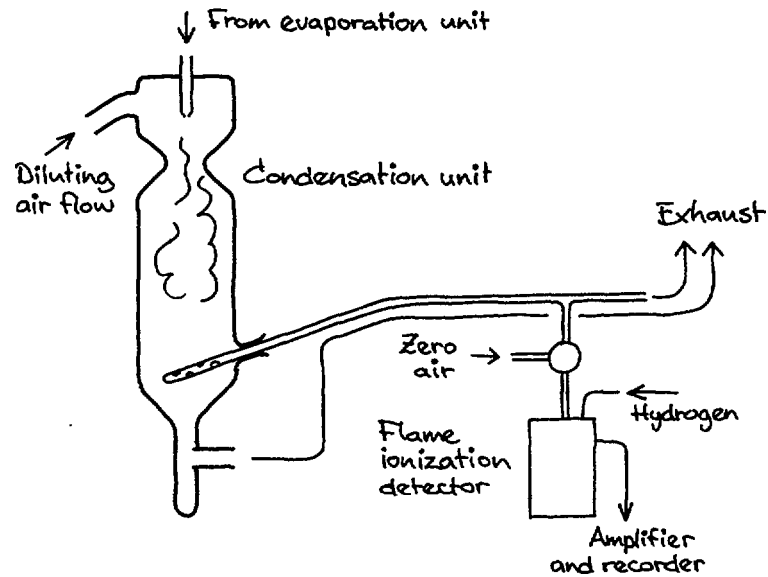


Fig 5.3 Connection of the flame ionization detector to the evaporation-condensation unit.

The observed ionization current is plotted against hydrocarbon concentration, Figure 5.4.

The constant k_{HC} in the expression

$$I_{ion} = K_{HC} \cdot c_{HC}$$

has been calculated. The results are as follows:

			K_{HC_3} A m ³ /kg
Manufacturer (Foa)			$2.14 \cdot 10^{-5}$
Calibration with propane	1974-11-25		$2.14 \cdot 10^{-5}$
Calibration with propane	1976-01-27		$2.24 \cdot 10^{-5}$
Calibration with propane	1976-01-29		$2.44 \cdot 10^{-5}$
Measurements on oil N	1976-01-28--29		$2.1 \cdot 10^{-5}$
Measurements on oil O	1976-02-02		$1.9 \cdot 10^{-5}$

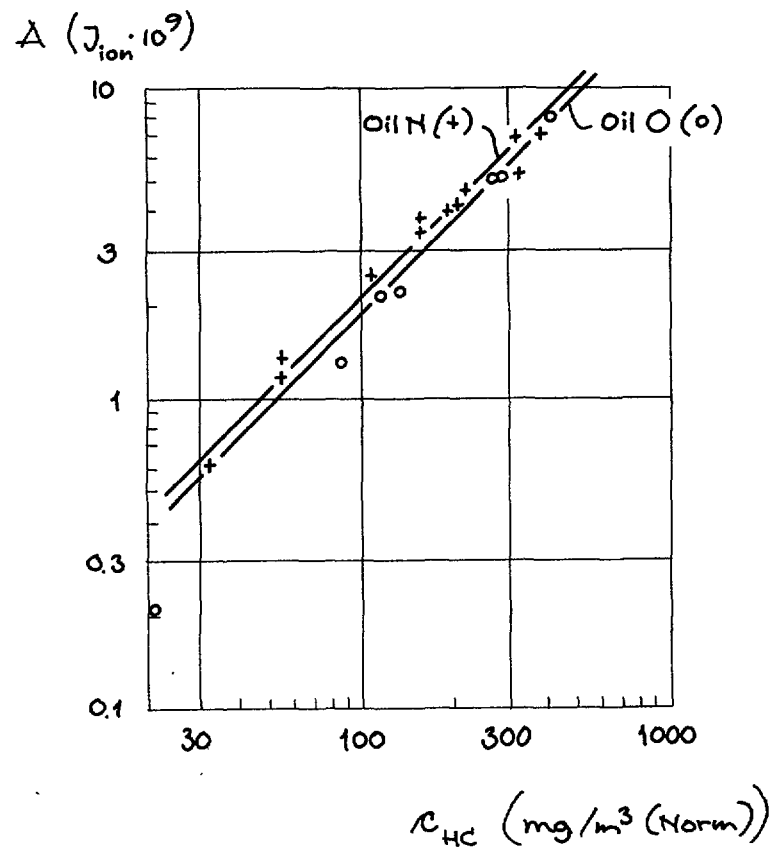


Fig 5.4 Observed ionization current as a function of oil concentration in sample flow.
Oven wall temperature 325°C.
Oven air temperature 295°C.
Oven air flow 100 ml (Norm)/s.
Diluting and cooling air flow 6 l(Norm)s.

Compared with the most recent propane calibrations, it seems that the flame ionization detector indicates on oil concentration 13 - 20 % lower than expected.

Unevaporated oil and wall losses in the condensation unit are collected at the bottom of the condensation unit. Very little oil was found here.

Losses in the transport from the condensation unit to the flame ionization detector cannot be evaluated, but might have had some influence.

There is also the possibility that the flame ionization detector has a lower sensibility to (possibly cracked and oxidized) oil than to propane.

The propane used for calibration may have partly oxidized in its steel container, and the calibration of 1974 might be more correct. In

such case there is much better agreement between observed and expected response to oil mist.

Further examination of this method of sample preparation will no doubt disclose the reason for observed discrepancies, but it seems already clear that the method can be used.

6. NOTES ON CONTINUED INVESTIGATIONS

Principle of measurement

Originally this project was aimed at the design of a cheap, easily applied instrument for oil and water contamination in compressed air lines. After having considered a number of possible principles, it was decided to employ sampling, with sample transport to the instruments proper. As is evidenced by this report, this approach involved some difficulties. These hindrances were surmounted, but it is still desirable to develop some other principle which does not include sampling.

Sampling

The samplers tested have been designed to provide information not only on the total flow of contaminants, but also on the mode of transport. If this information is not needed, the wall flow sampler can be excluded, getting the wall flow in the "coarse, air-borne" sampler.

The samplers for air-borne material have not been as thoroughly tested as the wall flow sampler. Here some work remains to be done.

Sample transport

As pointed out earlier, the "fine, air-borne" sampling chain does not work properly at low concentrations because the collected small amounts of liquid do not move in the sampling line. Especially at filter testing, the concentration of liquid downstream of the filter is very low. It is believed that a heated sampling line would also make filter testing possible with the present equipment.

Instruments

The humidity meter employed did not function to satisfaction. It is advisable to incorporate in an installation some means for calibration.

This could be, e.g., a manual dew-point meter, or a humid air generator.

The indicating reagent tubes tested proved to be very handy for moderately dry air. To simplify their use, and to extend the range of measurement to very dry air, a unit comprising a pressure containment for the tube should be developed, and also a sample volume meter.

The flame ionization detector functioned satisfactorily. But it is a complicated instrument, requiring a skilled operator. Its range of measurement does not extend to the rather high concentrations sometimes encountered in the sample air stream. In cases where highest sensitivity is not necessary and liquid water is absent, a catalytic combustion instrument (a kind of thermal analyzer) might be more suitable.

In conclusion, much work still remains to be done on the subject of compressed air contaminant measurement. Specifically, it should be noted that considerable savings could be made if one or more contaminant limits of Table 1:1 could be relaxed. If, for example, the liquid phase could be excluded, sampling would be much simplified. Or, if oil (water) were absent, the measurement of water (oil) could probably be made with simpler equipment. The work should thus be directed to more specific conditions and applications, e.g.

- test of filter efficiency
- test of dryer efficiency
- measurements on workplace air
- oil entrained from compressors
- air quality assurance in the food industry
- oil mist lubrication

7. REFERENCES

1. Additives
Von D Christakudis u a Hrsg von H Prinzler E W Berghoff.
Deutscher Verl f Grundstoffindustrie VEB, Leipzig 1966.
2. BAKER O
Simultaneous flow of oil and gas.
Oil gas J 53 (1954) p 185.
3. BRAUER H
Grundlagen der Einphasen- und Merhphasenströmungen.
Verlag Sauerländer, Frankfurt am Main 1971.
4. CIBULA G
Die Oxydation bei Schmierölen.
Mineralöltech 11 (1966) p 8.
5. FROSTLING H and BRANTTE A
A Mobile analysis instrument for the measurement of organic
vapours and aerosols in air.
J Phys E Sci instrum 1972 (5) p 251.
6. GOVIER G W and AZIZ K
The flow of complex mixtures in pipes. New York 1972.
7. GRUSE W A and STEVENS D R
Chemical Technology of petroleum. 3rd ed New York 1960.
8. HUHN J and WOLF J
Zweiphasenströmung. Gasförmig/flüssig. Leipzig 1975.
9. ISHII M
Thermo-fluid dynamic theory of two-phase flow. Paris 1975.
10. JASON A C
Some properties and limitations of the aluminium oxide hygro-
meter.
Humidity and moisture. Ed by Wexler, New York 1965 Vol 1 p 372.
11. LEVIN L M
The intake of aerosol samples.
Bull Acad Sci. USSR Geophys Ser 1957:7 p 87.
12. LEVY S
Prediction of two-phase annular flow with liquid entrainment.
Int J Heat Mass Transfer 9(1966) p 171.
13. MERCER T T
Aerosol technology in hazard evaluation. New York 1973.
14. MUNO H
Das Transportverhalten von Ölnebel in pneumatischen Verteiler-
systemen. Mainz 1973.

15. NORMAN W S and McINTYRE V
heat transfer to a liquid film on a vertical surface.
Trans Inst Chem Eng 38(1960) p 301.
16. QUANDT E
Analysis of gas-liquid flow patterns.
Chem Eng Progr Symp Ser 61(1965)57 p 128.
17. SCHLICHTING H
Grenzschicht - Theorie. Karlsruhe 1965.
18. SCOTT G
Atmospheric oxidation and antioxidants. Amsterdam 1966.
19. SWELL A P
How much oil is in your air system?
Power 119(1975)10 p 39.
20. MORGAN P G
The measurement of oil in compressed air lines.
Compress air Hydraul 27(1962)312 p 98.
21. EVANS A P
Sampling and analyzing of high pressure gas streams for lubricant content.
J Amer Ass Contam Contr 4(1965) July p 10.
22. CGA specification G-7. 1.
Commodity specifications for air. Compressed Gas Association, Inc, New York 1973.
23. HUYGHE J and MINK T Q
Ecoulement en tube d' un mélange de liquide et de gaz en régime annulaire dispersé: Mesure du débit de liquide en film à la paroi.
C R Acad Sci 260(1965) p 2405.
24. ISO
International organization for standardization.
Compressed non-breathing air for use in aircraft.
ISO 2434-1973(E).
25. DIN
Deutsche Normen.
Druckluft (Pressluft) für Atemgeräte.
DIN 3188. Januari 1974.
26. SITTEL P
Methoden der Ölnebel-Erzeugung und - Vermessung.
Diss Mainz 1970.

LIST OF PUBLISHED AE-REPORTS

1-440 (See back cover earlier reports.)

441. Neutron capture gamma ray cross sections for Ta, Ag, In and Au between 30 and 175 keV. By J. Hellström and S. Beshai. 1971. 30 p. Sw. cr. 15:--.
442. Thermodynamical properties of the solidified rare gases. By I. Ebbsjö. 1971. 46 p. Sw. cr. 15:--.
443. Fast neutron radiative capture cross sections for some important standards from 30 keV to 1.5 MeV. By J. Hellström. 1971. 22 p. Sw. cr. 15:--.
444. A Ge (Li) bore hole probe for in situ gamma ray spectrometry. By A. Lauber and O. Landström. 1971. 26 p. Sw. cr. 15:--.
445. Neutron inelastic scattering study of liquid argon. By K. Sköld, J. M. Rowe, G. Ostrowski and P. D. Randolph. 1972. 62 p. Sw. cr. 15:--.
446. Personnel dosimetry at Studsvik during 1970. By L. Hedlin and C.-O. Widell. 1972. 8 p. Sw. cr. 15:--.
447. On the action of a rotating magnetic field on a conducting liquid. By E. Dahlberg. 1972. 60 p. Sw. cr. 15:--.
448. Low grade heat from thermal electricity production. Quantity, worth and possible utilisation in Sweden. By J. Christensen. 1972. 102 p. Sw. cr. 15:--.
449. Personnel dosimetry at Studsvik during 1971. By L. Hedlin and C.-O. Widell. 1972. 8 p. Sw. cr. 15:--.
450. Deposition of aerosol particles in electrically charged membrane filters. By L. Ström. 1972. 60 p. Sw. cr. 15:--.
451. Depth distribution studies of carbon in steel surfaces by means of charged particle activation analysis with an account of heat and diffusion effects in the sample. By D. Brune, J. Lorenzen and E. Witalis. 1972. 46 p. Sw. cr. 15:--.
452. Fast neutron elastic scattering experiments. By M. Salama. 1972. 98 p. Sw. cr. 15:--.
453. Progress report 1971. Nuclear chemistry. 1972. 21 p. Sw. cr. 15:--.
454. Measurement of bone mineral content using radiation sources. An annotated bibliography. By P. Schmeling. 1972. 64 p. Sw. cr. 15:--.
454. Measurement of bone mineral content using radiation sources. An annotated bibliography. Suppl. 1. By P. Schmeling. 1974. 26 p. Sw. cr. 20:--.
455. Long-term test of self-powered detectors in HBWR. By M. Brakas, O. Strindberg and B. Söderlund. 24 p. 1972. Sw. cr. 15:--.
456. Measurement of the effective delayed neutron fraction in three different FR0-cores. By L. Moberg and J. Kockum. 1972. Sw. cr. 15:--.
457. Applications of magnetohydrodynamics in the metal industry. By T. Robinson, J. Braun and S. Linder. 1972. 42 p. Sw. cr. 15:--.
458. Accuracy and precision studies of a radiochemical multielement method for activation analysis in the field of life sciences. By K. Samsahl. 1972. 20 p. Sw. cr. 15:--.
459. Temperature increments from deposits on heat transfer surfaces: the thermal resistivity and thermal conductivity of deposits of magnetite, calcium hydroxy apatite, humus and copper oxides. By T. Kelén and J. Arvesen. 1972. 68 p. Sw. cr. 15:--.
460. Ionization of a high-pressure gas flow in a longitudinal discharge. By S. Palmgren. 1972. 20 p. Sw. cr. 15:--.
461. The caustic stress corrosion cracking of alloyed steels - an electrochemical study. By L. Dahl, T. Dahlgren and N. Lagmyr. 1972. 43 p. Sw. cr. 15:--.
462. Electrodeposition of "point" Cu^{125} roentgen sources. By P. Beronius, B. Johansson and R. Söremark. 1972. 12 p. Sw. cr. 15:--.
463. A twin large-area proportional flow counter for the assay of plutonium in human lungs. By R. C. Sharma, I. Nilsson and L. Lindgren. 1972. 50 p. Sw. cr. 15:--.
464. Measurements and analysis of gamma heating in the R2 core. By R. Carlsson and L. G. Larsson. 1972. 34 p. Sw. cr. 15:--.
465. Determination of oxygen in zircaloy surfaces by means of charged particle activation analysis. By J. Lorenzen and D. Brune. 1972. 18 p. Sw. cr. 15:--.
466. Neutron activation of liquid samples at low temperature in reactors with reference to nuclear chemistry. By D. Brune. 1972. 8 p. Sw. cr. 15:--.
467. Irradiation facilities for coated particle fuel testing in the Studsvik R2 reactor. By S. Sandklef. 1973. 28 p. Sw. cr. 20:--.
468. Neutron absorber techniques developed in the Studsvik R2 reactor. By R. Bodh and S. Sandklef. 1973. 26 p. Sw. cr. 20:--.
469. A radiochemical machine for the analysis of Cd, Cr, Cu, Mo and Zn. By K. Samsahl, P. O. Wester, G. Blomqvist. 1973. 13 p. Sw. cr. 20:--.
470. Proton pulse radiolysis. By H. C. Christensen, G. Nilsson, T. Reitberger and K.-Å. Thuomas. 1973. 26 p. Sw. cr. 20:--.
471. Progress report 1972. Nuclear chemistry. 1973. 28 p. Sw. cr. 20:--.
472. An automatic sampling station for fission gas analysis. By S. Sandklef and P. Svensson. 1973. 52 p. Sw. cr. 20:--.
473. Selective step scanning: a simple means of automating the Philips diffractometer for studies of line profiles and residual stress. By A. Brown and S. Å. Lindh. 1973. 38 p. Sw. cr. 20:--.
474. Radiation damage in CaF_2 and BaF_2 investigated by the channeling technique. By R. Hellborg and G. Skog. 1973. 38 p. Sw. cr. 20:--.
475. A survey of applied instrument systems for use with light water reactor-contaminants. By H. Tuxen-Meyer. 1973. 20 p. Sw. cr. 20:--.
476. Excitation functions for charged particle induced reactions in light elements at low projectile energies. By J. Lorenzen and D. Brune. 1973. 154 p. Sw. cr. 20:--.
477. Studies of redox equilibria at elevated temperatures 3. Oxide/oxide and oxide/metal couples of iron, nickel, copper, silver, mercury and antimony in aqueous systems up to 100°C. By Karin Johansson, Kerstin Johansson and Derek Lewis. 1973. 42 p. Sw. cr. 20:--.
478. Irradiation facilities for LWR fuel testing in the Studsvik R2 reactor. By S. Sandklef and H. Tomani. 1973. 30 p. Sw. cr. 20:--.
479. Systematics in the (p,xn) and (p,pxn) reaction cross sections. By L. Jéki. 1973. 14 p. Sw. cr. 20:--.
480. Axial and transverse momentum balance in subchannel analysis. By S. Z. Rouhani. 1973. 58 p. Sw. cr. 20:--.
481. Neutron inelastic scattering cross sections in the energy range 2 to 4.5 MeV. Measurements and calculations. By M. A. Etemad. 1973. 62 p. Sw. cr. 20:--.
482. Neutron elastic scattering measurements at 7.0 MeV. By M. A. Etemad. 1973. 28 p. Sw. cr. 20:--.
483. Zooplankton in Tvären 1961-1963. By E. Almquist. 1973. 50 p. Sw. cr. 20:--.
484. Neutron radiography at the Studsvik R2-0 reactor. By I. Gustafsson and E. Sokolowski. 1974. 54 p. Sw. cr. 20:--.

ISBN 91-7010-006-3

485. Optical model calculations of fast neutron elastic scattering cross sections for some reactor materials. By M. A. Etemad. 1974. 165 p. Sw. cr. 20:--.
486. High cycle fatigue crack growth of two zirconium alloys. By V. S. Rao. 1974. 30 p. Sw. cr. 20:--.
487. Studies of turbulent flow parallel to a rod bundle of triangular array. By B. Kjellström. 1974. 190 p. Sw. cr. 20:--.
488. A critical analysis of the ring expansion test on zircaloy cladding tubes. By K. Pettersson. 1974. 8 p. Sw. cr. 20:--.
489. Bone mineral determinations. Proceedings of the symposium on bone mineral determinations held in Stockholm-Studsvik, Sweden, 27-29 May 1974. Vol. 1. Presented papers. 1974. 170 p. Sw. cr. 20:--.
489. Bone mineral determinations. Proceedings of the symposium on bone mineral determinations held in Stockholm-Studsvik, Sweden, 27-29 May 1974. Vol. 2. Presented papers (cont.) and group discussions. 1974. 200 p. Sw. cr. 20:--.
489. Bone mineral determinations. Proceedings of the symposium on bone mineral determinations held in Stockholm-Studsvik, Sweden, 27-29 May 1974. Vol. 3. Bibliography on bone morphometry and densitometry in man. By A. Horsman and M. Simpson. 1974. 112 p. Sw. cr. 20:--.
490. The over-power ramp fuel failure phenomenon and its burn-up dependence - need of systematic, relevant and accurate irradiation investigations. - Program proposal. By H. Mogard. 1974. Sw. cr. 20:--.
491. Phonon anharmonicity of germanium in the temperature range 80-880 K. By G. Nelín and G. Nilsson. 1974. 28 p. Sw. cr. 20:--.
492. Harmonic lattice dynamics of germanium. By G. Nelín. 1974. 32 p. Sw. cr. 20:--.
493. Diffusion of hydrogen in the β -phase of Pd-H studied by small energy transfer neutron scattering. By G. Nelín and K. Sköld. 1974. 28 p. Sw. cr. 20:--.
494. High temperature thermocouple applications in the R2-reactor, Studsvik. By B. Rohne. 1974. 20 p. Sw. cr. 20:--.
495. Estimation of the rate of sensitization in nickel base alloys. By J. Wiberg. 1974. 14 p. Sw. cr. 20:--.
496. A hort-el-complex in Sweden. By J. Christensen. 1974. 82 p. Sw. cr. 20:--.
497. Effect of wall friction and vortex generation on radial void distribution - the wall-vortex effect. By Z. Rouhani. 1974. 36 p. Sw. cr. 20:--.
498. The deposition kinetics of calcium hydroxy apatite on heat transfer surfaces at boiling. By T. Kelén and R. Gustafsson. 1974. 30 p. Sw. cr. 20:--.
499. Observations of phases and volume changes during precipitation of hydride in zirconium alloys. By G. Östberg, H. Bergqvist, K. Pettersson, R. Attermo, K. Norrgård, L.-G. Jansson and K. Malén. 1974. 16 p. Sw. cr. 20:--.
500. X-ray elastic constants for cubic materials. By K. Malén. 1974. 25 p. Sw. cr. 20:--.
501. Electromagnetic screening and skin-current distribution with magnetic and non-magnetic conductors. By E. Dahlberg. 1974. 44 p. Sw. cr. 20:--.
502. Depth distribution studies of carbon, oxygen and nitrogen in metal surfaces by means of neutron spectrometry. By J. Lorenzen. 1975. 54 p. Sw. cr. 20:--.
503. A systematic study of neutron inelastic scattering in the energy range 2.0 to 4.5 MeV. By E. Almén-Ramström. 1975. 108 p. Sw. cr. 20:--.
504. Analysis of EPR with large quadrupole interaction. By K.-Å. Thuomas. 1975. 28 p. Sw. cr. 20:--.
505. Observations on deformation systems in zircaloy-2 deformed at room temperature. By K. Pettersson and H. Bergqvist. 1975. 20 p. Sw. cr. 20:--.
506. Study of a tritium-fueled battery utilizing the difference of workfunction between electrodes. By J. Braun. 1975. 20 p. Sw. cr. 20:--.
507. X-ray Characterization of non-equilibrium solid solutions. By A. Brown and O. Rosdahl. 1975. 30 p. Sw. cr. 20:--.
508. Statistic performance of dichromatic scanners for absorptometric determination of bone mineral content using low energy gamma rays. By E. Dissing. 1975. 12 p. Sw. cr. 20:--.
509. Fast reactor blanket experiments in FR0. By T. L. Andersson, R. Håkansson, R. Richmond and P. Stevens. 1976. 51 p. Sw. cr. 20:--.
510. Two phase sintering of UO_2 -20 CeO_2 . A homogenization model for mixed-oxide fuel pellets. By Allan Brown. 1976. 72 p. Sw. cr. 20:--.
511. Methods for sampling and measurement of compressed air contaminants. By L. Ström. 1976. 46 p. Sw. cr. 20:--.

List of published AES-reports (In Swedish)

1. Analysis by means of gamma spectrometry. By D. Brune. 1961. 10 p. Sw. cr. 6:--.
2. Irradiation changes and neutron atmosphere in reactor pressure vessels - some points of view. By M. Grounes. 1962. 33 p. Sw. cr. 6:--.
3. Study of the elongation limit in mild steel. By G. Östberg and R. Attermo. 1963. 17 p. Sw. cr. 6:--.
4. Technical purchasing in the reactor field. By Erik Jonson. 1963. 64 p. Sw. cr. 8:--.
5. Ågesta nuclear power station. Summary of technical data, descriptions, etc. for the reactor. By B. Lilliehöök. 1964. 336 p. Sw. cr. 15:--.
6. Atom Day 1965. Summary of lectures and discussions. By S. Sandström. 1966. 321 p. Sw. cr. 15:--.
7. Building materials containing radium considered from the radiation protection point of view. By Stig O. W. Bergström and Tor Wahlberg. 1967. 26 p. Sw. cr. 10:--.
8. Uranium market. 1971. 30 p. Sw. cr. 15:--.
9. Radiography day at Studsvik. Tuesday 27 april 1971. Arranged by AB Atomenergi, IVA's Committee for nondestructive testing and TRC AB. 1971. 102 p. Sw. cr. 15:--.
10. The supply of enriched uranium. By M. Mårtensson. 1972. 53 p. Sw. cr. 15:--.
11. Fire studies of plastic-insulated electric cables, sealing lead-in wires and switch gear cubicles and floors. 1973. 117 p. Sw. cr. 35:--.
12. Soviet-Swedish symposium on reactor safety problems. Studsvik, march 5-7, 1973. Part 1. Swedish papers. 1973. 109 p. Sw. cr. 20:--.
12. Soviet-Swedish symposium on reactor safety problems. Studsvik, march 5-7, 1973. Part 2. Soviet papers. 1973. 120 p. Sw. cr. 20:--.
13. International and national organizations within the nuclear energy field. By S. Sandström. 1975. 24 p. Sw. cr. 20:--.
14. Energy analysis and power growth patterns. By K. Jirlow. 1975. 44 p. Sw. cr. 20:--.

Additional copies available from the Library of AB Atomenergi, Fack, S-611 01 Nyköping 1, Sweden.